DEPARTMENT OF TRANSPORTATION

Development of Biochar Specification Criteria as Soil Amendment for Slopes, Conveyances and Stormwater Treatment Systems (Phase 1)

Brian Barry, Principal Investigator
Natural Resources Research Institute
University of Minnesota

July 2025

Research Project
Final Report 2025-36

LRRB
LOCAL ROAD RESEARCH BOARD

To get this document in an alternative format or language, please call 651-366-4720 (711 or 1-800-627-3529 for MN Relay). You can also email your request to ADArequest.dot@state.mn.us. Please make your request at least two weeks before you need the document.

Technical Report Documentation Page

1. Report No.	2.	3. Recipients Accession No.
MN 2025-36		

4. Title and Subtitle	5. Report Date
Development of Biochar Specification Criteria as Soil Amendment for Slopes, Conveyances and Stormwater Treatment Systems (Phase 1)	July 2025
	6.

7. Author(s)	8. Performing Organization Report No.
Brian Barry, Tadele Haile, Bridget Ulrich & Matt Young	

9. Performing Organization Name and Address	10. Project/Task/Work Unit No.
Natural Resources Research Institute University of Minnesota - Duluth 5013 Miller Trunk Hwy. Duluth, MN 55811	11. Contract (C) or Grant (G) No. (c) 1036342 (wo)87

12. Sponsoring Organization Name and Address	13. Type of Report and Period Covered
Minnesota Department of Transportation Office of Research & Innovation 395 John Ireland Boulevard, MS 330 St. Paul, Minnesota 55155-1899	Final Report
	14. Sponsoring Agency Code

15. Supplementary Notes

http://mdl.mndot.gov/

16. Abstract (Limit: 250 words)

The objective of this project is to develop knowledge, tools, and protocols to inform best practice standards for effective implementation of biochar in bioretention systems (BRSs) for treating roadway runoff. This project will be performed in two phases, with the first phase (this report) focusing on biochar production, characterization, and contaminant sorption performance. Results from the first phase will inform decisions for the second phase which will look at vegetation growth studies and soil hydrology evaluations. We anticipate the primary project output (following completion of Phase 2) to be a tool or protocol (e.g., a decision-making matrix) to provide standardized guidance for best practices regarding the practical implementation of biochar in BRSs treating roadway runoff. The work plan for Phase 1 is presented herein, which will result in following outputs:

1. Recommendations for locally available, suitable biomass feedstocks and feedstock-specific pyrolysis conditions which can be reproduced at scale.
2. Biochar physical property specification criteria associated with contaminant-removal targets which can be assessed at reasonable costs.
3. Protocols for screening-level contaminant-removal performance tests based on broadly accessible materials and methods.
4. Plans for further evaluations to verify treatment performance and evaluate hydraulic and soil health effects, to be proposed as a part of Phase 2 investigations

17. Document Analysis/Descriptors	18. Availability Statement
Detention basins, Runoff, Contaminants, Engineering soils	No restrictions. Document available from: National Technical Information Services, Alexandria, Virginia 22312

19. Security Class (this report)	20. Security Class (this page)	21. No. of Pages	22. Price
Unclassified	Unclassified	58	

Development of Biochar Specification Criteria as Soil Amendment for Slopes, Conveyances and Stormwater Treatment Systems (Phase 1)

Final Report

Prepared by:

Brian Barry, Tadele Haile, Bridget Ulrich & Matt Young
Natural Resources Research Institute
University of Minnesota-Duluth

July 2025

Published by:

Minnesota Department of Transportation
Office of Research & Innovation
395 John Ireland Boulevard, MS 330
St. Paul, Minnesota 55155-1899

ACKNOWLEDGEMENT

The research team is grateful for the funding provided by the Minnesota Department of Transportation (MnDOT) for this project. Special thanks are due to Dwayne Stenlund for his significant contribution serving as the Technical Lead and Barbara Fraley for her significant contribution serving as the Project Coordinator. We also extend our appreciation to the members of the project's Technical Advisory Panel (TAP) for their invaluable guidance, time and expertise. TAP members include Joanne Boettcher, Alyssa Boock, Jim Doten, Blaize Holden, Bryce Johnson, Paul Jurek, Ed Matthiesen, Mark Polega, Warren Tuel, Kelsi Ustipak, Brandon Wisner, Brent Rusco, and Julie Swiler.

The research team would also like to thank Lee Harnell (Proctor Builders Supply) for donating all the emerald ash borer infested ash trees used for biochar production.

Table of Contents

List of Figures

List of Tables

Executive Summary

Stormwater runoff from roadways is a major contributor of nonpoint source pollution of Minnesota watersheds and carries contaminants such as dissolved metals and fossil fuel hydrocarbons (e.g., motor oil) (Lundy et al, 2012). Roadway swales and basins, when constructed with high permeability materials, act as low impact bioretention systems (BRSs). In addition to high permeable materials, swales may be constructed with fillers composed of organic materials and local soils (Xiong, et al, 2022). Although current BRS designs have demonstrated adequate performance in many aspects, the design has room for improvement in a) increasing the lifespan of the BRSs, b) decreasing the costs of BRS construction, c) reducing peak flow rates during intense rain events, d) improving select contaminant removal performance and e) improving revegetation and deep root growth on swales. This project will explore the incorporation of biochar into engineered soils in BRSs and will be evaluated for how its integration impacts the previously mentioned shortcomings (a-e).

In this portion of the project (Phase 1), we developed recommendations for the requisite biochar physicochemical properties required for acceptable stormwater contaminant removal. These recommendations are accompanied with guidance for biochar producers and end-users on how to best achieve these desired properties (e.g., biomass feedstock choice and pyrolysis conditions) and how to best test for these desirable biochar attributes. The results from Phase 1 will inform decisions for Phase 2 of this project, where the focus will shift to field soil hydrology tests and development of construction designs for the implementation of biochar into BRSs. With the reminder that our "final" recommendations must consider data from future work in Phase 2 and that the current recommendations here may be impacted, a summary of our current conclusions and recommendations are as follows:

Recommended biochar properties, feedstock choice and testing recommendations:

1) **An $H:C_{org}$ (hydrogen to organic carbon) molar ratio of ≤ 0.2.** To achieve this, a highest thermal treatment (HTT) temperature (aka maximum pyrolysis temperature) of 675 °C must be met or exceeded during biochar production. It should be noted that a $H:C_{org}$ value of 0.3 (HTT of ~600 °C) is adequate for dissolved metal contamination, but for hydrocarbon sorption, a higher temperature char significantly improves performance.

    a. **Testing Recommendations:** There are several analytical service labs across the country that offer the required testing necessary to calculate the $H:C_{org}$ molar ratio. Ultimate analysis utilizes elemental combustion (aka CHN(O)S analysis) to determine the total %C and %H by weight in the bulk sample. A separate aliquot of the sample is ashed in a muffle furnace at 550 °C (critical not to exceed 550 °C as to not decompose the carbonates) and the resulting ash is also analyzed by combustion analysis. The carbon present in the ash is referred to as "inorganic carbon," and once this has been determined one can subtract the inorganic carbon content from the total carbon allowing for the "organic carbon" content to be determined. While this lab is only one of many that can offer this service, we recommend using Timber Products Inspection Inc. (Conyers, GA) as they specialize in analysis of biomass.

2) **Extractives Content of ≤ 0.25%.** The clean separation of condensable organics (tars) from the biochar product is often very challenging as ~50% by weight of the biomass results in volatiles. Tar build-up, particularly when feed rates are increased, can present real challenges and biochar products very frequently have unwanted tars redeposited on the biochar surface. This surface sorbed tars can decrease contamination removal performance and can even lead to introducing unwanted mobile organics into the environment.

    a. **Testing Recommendations:** This analysis is performed by extracting a 10-20 g sample of dry biochar with a 50/50 (by volume) solvent mixture of benzene and ethanol in an overnight (15 h) Soxhlet extraction. Following extraction, the supernatant has its volatiles removed via rotary evaporation and the total weight of the extractives is reported as a weight percentage relative to the mass of biochar sample used for extraction. This test is not offered by commercial analytical labs but is a very simple procedure that does not require expensive instrumentation. In instances when this test is not available to the practitioner for whatever reason, there is a simpler, qualitative assessment that can be performed. First, the biochar should be odorless. Upon wafting the sample, if any smell reminiscent of campfire is detected, the sample likely exceeds the 0.25% extractives content threshold. Second, if you take a small handful of biochar and rub it between your hands, there should be no discernable oily feeling in your hands. An odorless biochar that leaves no oily residue behind on your hands is a good sign that the volatiles were properly separated from the biochar product during production.

3) **Presence of adequate pore volumes (≥ 0.40 mL/g) in the "vascular" pore diameter range (500-80,000 nm).** Biochar products do not receive additional "activation" processing (widening of micropores into mesopores) like activated carbon products do and typically have very small pore volumes in the mesoporous region. However, unlike activated carbons, biochars made from plant feedstocks (for the most part) will have significant pore volumes in the vascular range (*pseudo*-macroporous). This allows biochars with appropriate vascular pore volumes to perform as well as activated carbons regarding uptake of the contaminants being investigated here.

    a. **Testing Recommendations:** There are several ways to assess the vascular porosity of a biochar sample. The most reliable test is a quantitative assessment employing a mercury intrusion porosimeter (MIP) and is a test offered by many commercial analytical labs. This test allows for the quantification of pore volume in the recommended 500-80,000 nm pore diameter range and should exceed 0.40 mL/g. Our lab has a MIP instrument and so we have not had to rely on external labs, and as such cannot recommend a specific commercial lab for these tests. Another way to assess the vascular porosity is through imaging. Scanning electron microscopy (SEM) can allow for the visual inspection of the surface where the vascular pores, if present, are plainly obvious (several examples are shown later in report for reference) and the diameters of the pores can be easily measured. A third option is to perform a water holding capacity (WHC) test. This is a very simple test which requires basic laboratory implements (Falcon tubes, filter paper, scale etc.) and can provide insight into the presence of vascular pores but cannot identify them outright. The water holding

capacity that biochar's possess is largely due to the presence of right-sized pores for water filling and should result in a WHC of at least 3 g of sorbed water per gram of biochar sample (g/g). Finally, another option, coke reactivity index (CRI) is under development by our lab and allows for the approximate total pore volume (TPV) to be determined. This test is detailed subsequently in this report and outlines how the TPV correlates to the CRI.

4) **Woody feedstocks.** Shipping in biochar from afar is neither economically or environmentally rational, so we must focus on local biomass resources in Minnesota, and even better if we can identify suitable biomass feedstock which are considered waste (e.g., pest infested ash or spruce, sawmill residues, or fuels removed in fire mitigation efforts). Minnesota has no shortage of woody biomass waste which is not being utilized and, given it is ideal for producing biochar with significant vascular porosity, it is the obvious choice. Other typical feedstocks for biochar production are grasses (e.g., miscanthus), agricultural residues (e.g., corn stover) or even biosolids. While biochars from grasses and agricultural residues have shown l to have equal or higher porosities than woody biochars, the porosity comes from the micropores and mesopores and not from the more useful vascular pores. Biosolids do not produce biochars with suitable porosity for the application being explored here and could also be a source of contamination.

Significance of Research

While research looking into biochar's properties and application-specific performance are not uncommon, most of these studies have oversights that were not considered. These include: a) inadequate temperature probing and recording of pyrolysis conditions, b) utilization of an inappropriate specific surface area measurement technique (N_2 BET), c) lack of "regime-specific" total pore volume determinations and complete pore size distributions (PSDs), d) ash content evaluations performed at inappropriately high temperatures (typically 800 °C), e) small range of pyrolysis HTTs, and f) lack of control testing for performance comparisons to name a few.

One of the most critical aspects of this project was to have rigorously tight control of the kiln temperatures during pyrolysis. We produced biochar products at ten different HTTs ranging from 300 °C to 975 °C and each of these temperatures required its own heating calibration to ensure that the kiln temperature was stable at the selected HTT. An example plot showing the monitoring of kiln temperature during a pyrolysis run is presented later. The success of our kiln temperature control is apparent when plotting various metrics vs. HTT production temperature (namely proximate, ultimate and $H:C_{org}$), showing clear trends as the temperature is modified.

Lastly, our study utilized state-of-the-art measurements for complete PSDs. These onerous analyses require three separate experiments (N_2 absorption, CO_2 absorption, and MIP) to generate a single complete PSD plot covering the entire range of pore sizes present in biochar products. This method is rarely seen in the literature but is widely accepted as best practice. Additionally, we created a tool that allows us to choose the upper and lower limits of a pore diameter range of interest and quickly determine the pore volume in that range. This approach to analyzing PSDs was developed in our labs and allows us to identify meaningful trends when comparing PSD attributes to performance. The ability to compare user-defined, regime-specific pore volumes with their contamination uptake performance,

for example, is a powerful tool unique to this study and, we believe, represents a significant improvement in identifying performance-property relationships in biochar products.

Chapter 1: Introduction

1.1 Objectives

The objective of this project is to develop knowledge, tools, and protocols to inform best practice standards for effective implementation of biochar in BRSs for treating roadway runoff. This project will be performed in two phases, with the first phase (this report) focusing on biochar production, characterization, and contaminant sorption performance. Results from the first phase will inform decisions for the second phase which will look at vegetation growth studies, soil hydrology evaluations, and implementation guidance. We anticipate the primary project output (following completion of Phase 2) to be a tool or protocol (e.g., a decision-making matrix) to provide standardized guidance for best practices regarding the practical implementation of biochar in BRSs treating roadway runoff. The work plan for Phase 1 is presented herein, and discusses the following:

1) Recommendations for locally available, suitable biomass feedstocks and feedstock-specific pyrolysis conditions which can be reproduced at scale.
2) Biochar physical property specification criteria associated with contaminant-removal targets which can be assessed at reasonable costs.
3) Protocols for screening-level contaminant-removal performance tests based on broadly accessible materials and methods.
4) Plans for further evaluations to verify treatment performance and evaluate hydraulic and soil health effects, to be proposed as a part of Phase 2 investigations

1.2 Biomass Feedstock Selection and Acquisition

After much consideration and many conversations with our extensive network of biochar producers and practitioners, the first important decision which is necessary to describe, was the decision to pick a singular biomass feedstock type to use for all of Phase 1. This decision is reflective of both the technical lead (Dwayne Stenlund) and the principal investigator (Brian Barry) having a strong opinion that the suitability of biochar products for incorporation into bioretention systems (BRSs) should be reflective of the physicochemical analysis of the product and not dependent upon biomass identity. Additionally, drawing upon Dr. Barry's and Dr. Ulrich's (co-principal investigator) significant research experience examining the property-performance relationship of biochars in contaminant absorption applications, we decided that a woody biomass feedstock would be an ideal choice for this phase of the project. Considering that the state of Minnesota's biomass availabilities for biochar production are largely wood waste products, the selection of a wood-based feedstock was made even easier. Lastly, after consultation with entities we identified as being the closest to large-scale biochar production in the state of Minnesota (the City of Minneapolis and Carbon Alliance), it was determined that the most likely biomass feedstock to be employed in biochar production at rates that could accommodate major BRS construction projects is emerald ash borer infested ash trees. As such, we will use delimbed, chipped ash wood as the feedstock for all biochar products produced as part of this phase of the project.

1.3 Design of Experiment

The most impactful independent variable for biochar production is the highest temperature treatment (HTT), the maximum temperature the biomass feedstock is exposed to during pyrolysis, which effects the resulting biochar's physicochemical and performance properties. To this end, we will produce 10 ash biochar products with HTTs ranging from 300 to 975 °C with 75 °C increments between targeted HTTs. In producing these 10 samples, we will keep all other variables constant including: sample mass, sample preparation (sizing and drying), heating ramp rate, retention time at HTT, sweep gas composition (100% nitrogen) and cooling rate.

In addition to HTT, a second independent variable will be the introduction of 4% by volume oxygen into the sweep gas. A small addition of oxygen into the sweep gas results in a widening of the micro/mesopores in the resulting biochars which we hypothesize will have significant implications on the biochar's contaminant sorption performance (See Figure 1.1). Due to project limitations, oxygen will only be introduced to biochar productions at five HTTs (375 °C, 525 °C, 675 °C, 825 °C and 975 °C), resulting in a total of 15 unique biochar samples which can be seen in Table 1.1. It should be noted that all biochar production runs for each of the 15 samples will produce enough material for all physicochemical characterizations (performed by Dr. Barry's group) and for all contaminant sorption experiments (performed by Dr. Bridget Ulrich's group).

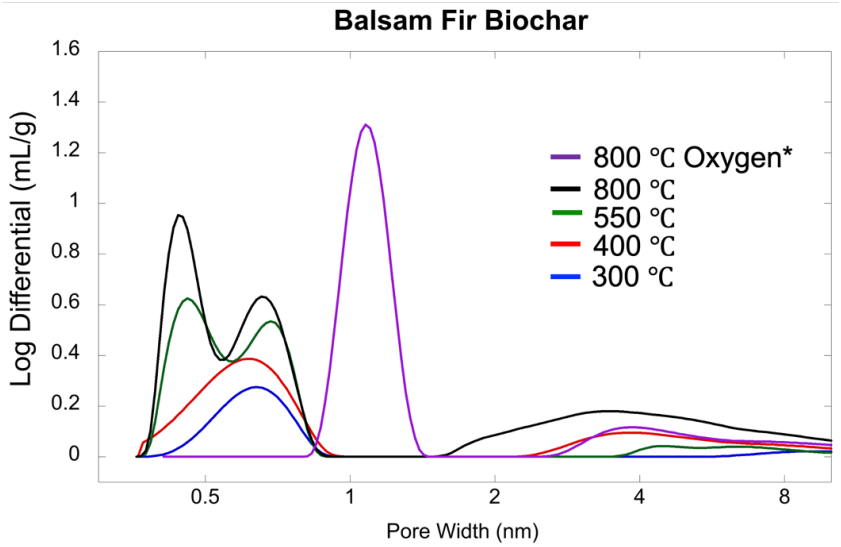

Figure 1.1 Pore size distributions of balsam fir biochar produced under nitrogen only (blue, red, green and black) and under 4% oxygen and 96% nitrogen (purple) highlighting the resulting widening of pores upon introduction of oxygen.

Table 1.1. List of pyrolysis conditions for all 15 samples produced

Sample Number	HTT (°C)	Sweep Gas Composition
1	300	100% N_2
2	375	100% N_2
3	375	96% N_2, 4% O_2
4	450	100% N_2
5	525	100% N_2
6	525	96% N_2, 4% O_2
7	600	100% N_2
8	675	100% N_2
9	675	96% N_2, 4% O_2
10	750	100% N_2
11	825	100% N_2
12	825	96% N_2, 4% O_2
13	900	100% N_2
14	975	100% N_2
15	975	96% N_2, 4% O_2

Chapter 2: Biochar Production

2.1 Commissioning and Calibration of New Biochar Production Kiln

The Materials & Bioeconomy research group at NRRI had just installed a new batch biochar kiln (tube furnace, see Figure 2.1 below) right before the start of this project. This was a useful asset to have in place as a single production run on this kiln will yield enough biochar for all necessary characterizations and sorption performance tests for each product. On one end of the tube, gas was flowed in from connected gas cylinders (either pure N_2, or 96% N_2/4% O_2) and drawn through the tube (reaction chamber) using an eductor connected to the opposite end of the tube. Additionally, the kiln was fit with a large, ice-cooled impinger bottle to condense and trap all organic volatiles generated as byproducts of the wood pyrolysis. The raw woody biomass (pre-dried overnight at 105 °C) chips were loaded into a custom-built perforated metal basket (See Figure 2.2 below) which had a small diameter tube running through the middle allowing for the introduction of a thermocouple so that we could monitor the temperature in the middle of the sample basket. Furthermore, the metal basket was constructed with metal veins spanning the center of the basket (thermocouple sleeve) from the edges of the basket to aide in heat transfer from the kiln heating coils to the center of the sample basket (biochar is a good insulator).

Since the active (heated) portion of the tube furnace measures four feet long, we found that a constant temperature across the entire sample basket required some experimentation, as the ends of the tube are slightly cooler than the center. The furnace is split into 3 horizontal zones, and by tweaking the temperatures in the two terminal zones, one can achieve a constant temperature across the length of the sample basket. For each targeted HTT, a calibration experiment was required whereby the set temperatures for each of the 3 zones (red, green and blue lines in Figure 2.3) was established for producing the right temperature across the volume of the sample basket. Temperatures from the thermocouple placed in the center of the sample basket (charge, see purple line in Figure 2.3) were monitored throughout the duration of the biochar production runs and we were able to achieve a variance in temperature of no more than ± 5 °C from the targeted temperature for all runs (see Figure 2.3). It should be noted that all samples were held at their HTT for a residence time of 80 minutes.

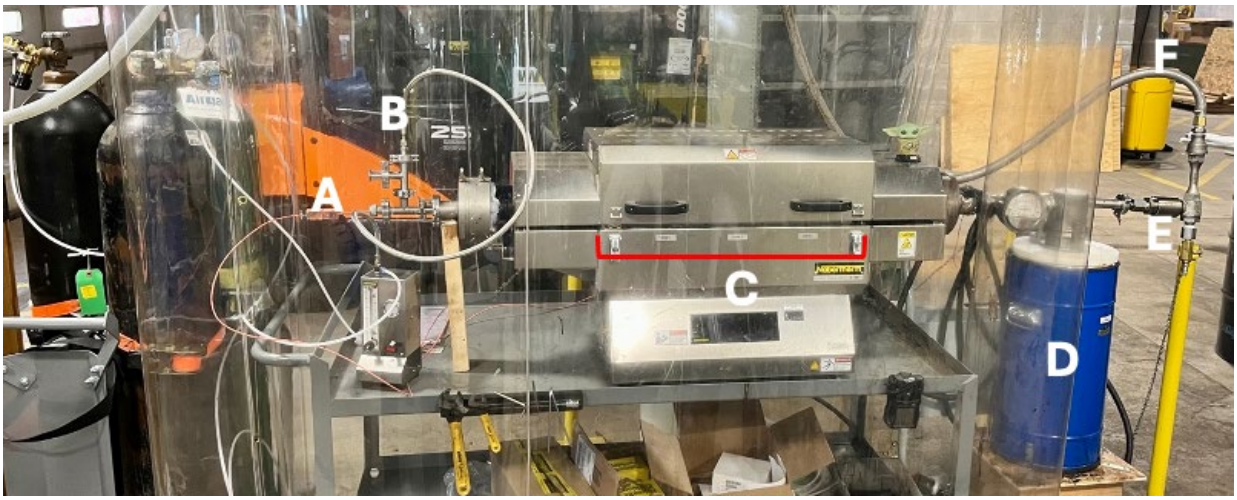

Figure 2.1 The biochar production kiln (batch tube furnace) used to produce all biochar products for Phase 1. A) Internal thermocouple which extends through the sample basket (see Figure 2) to the center of the tube furnace. B) Sweep gas inlet port. C) Heating zone of tube furnace, 26" long. D) Impinger bottle for condensing organic volatiles. E) Eductor used to draw sweep gas through the tube furnace. F) Exhaust line.

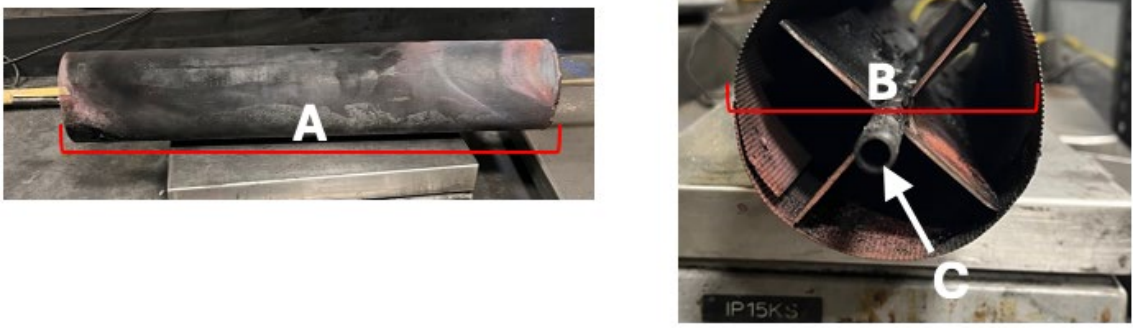

Figure 2.2 Images of the custom biochar basket used to hold material during pyrolysis. A) Side view of basket, 20" long. B) Diameter of basket, end-on view, 4". C) Thermocouple port.

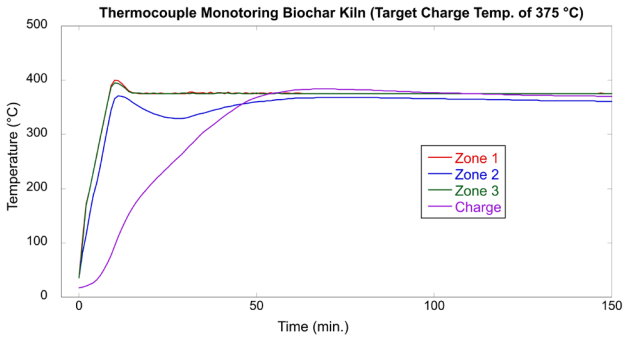

Figure 2.3 Kiln thermocouple temperature readings vs. time.

2.2 Biochar Production Details

Approximately 600 grams of dried, raw black ash chips (sized to between 3/16” and 3/4") were loaded into the sample basket and then the sample basket was placed in the center of the tube furnace. Once the thermocouple had been placed into the center of the sample basket, the tube was sealed and connected to the gas cylinders (sweep gas) and the impinger/eductor system on the opposite end of the tube. Samples were heated from room temperature to the HTT at a rate of ~0.5 °C/s (slow pyrolysis), and as previously stated, held at the HTT for 80 minutes prior to turning off the heating elements on the tube furnace. The material was allowed to cool naturally to room temperature under N_2 flow before retrieving the product from the kiln. For samples where 4% O_2 was introduced the sweep gas, this was done by opening a valve to the connected O_2 tank and the N_2 and O_2 would mix prior to entering the tube furnace. The valves were set up such that we could switch between N_2 only and an N_2/O_2 mixture simply by turning a single ¼ turn plug valve. To achieve the correct N_2/O_2 ratio, flow meters were used to calibrate the rate of gas introduction from each of the two cylinders prior to production runs. The N_2/O_2 mixture was only used as the sweep gas for 20 minutes of the total 80 minutes at HTT. All biochar products underwent milling and sizing post-production to accommodate the size requirements for characterization and sorption testing. This required two different sizings of -10/+20 mesh and -60/+270 mesh for each product produced (See Figure 2.4 below).

Figure 2.4 Images of a representative black ash biochar (525 °C HTT) product in three different sizings. As-produced (left). -10/+20 mesh (center). -60/+270 mesh (right).

Chapter 3: Biochar Characterization

3.1 Overview of Characterizations and decision to exclude cation exchange capacity testing from workplan

A full description of the biochar characterization workplan from the proposal is detailed in Appendix A. Since the proposal submission, a decision was made to forego the proposed cation exchange capacity (CEC) testing and an explanation for that decision can be seen below. Additionally, some biochar products and a series of coal and activated carbon products had additional testing (CRI and SEM) performed to compliment the observations form the results from the proposed characterizations. Below is a summary of the biochar characterizations performed over the course of the project:

1) Proximate and Ultimate Analysis
2) Extractives quantification
3) Complete Pore Size Distribution (PSD)
4) Water Holding Capacity
5) Butane Activity
6) SEM imaging (select samples only)
7) CRI (select samples only)

In this section, the results from all characterizations experiments will be presented. Along with presenting the data, context for why each of these experiments were chosen will be discussed.

Decision to exclude CEC from workplan: To quantify the CEC of a solid material there are many approaches, but they all involve suspending a solid sample (previously treated with acid to displace all metal cations with protons, followed by filtration) in an aqueous solution that was pre-loaded with some sort of dissolved cation. The cations in solution exchange with hydrogen atoms from the solid sample, releasing protons (H^+ cations) into the solution. The amount of protons released is quantified via pH titration and the CEC is expressed as centimoles of protons released per kg of solid sample (cmol/kg). Standard methods for determining CEC were first developed with soils being the media targeted for assessment. Soils, relative to both raw woody biomass and woody biochar, contain a significantly higher content of carboxyl (-COOH) functional groups, which are responsible for the cation exchange activity. In soils, the humic acids (primary constituent of soil organic matter) and fulvic acids are known to have ~4 and ~9 mmol of COOH per gram of material respectively for a total carboxyl content of ~13 mmol/g (Varadachari & Ghosh, 1984) while lignins (found in raw biomass) are known to have a carboxyl content of ~1.5 mmol/g (Junghans et al, 2020). Furthermore, upon pyrolysis (biochar production), the biomass undergoes decarboxylation and condensation reactions which further lower the carboxyl group content relative to the unpyrolized starting material.

For this project, since the biochar will be mixed in an engineered soil for deployment, it is important to consider how impactful the addition of biochar will be to the overall CEC of the biochar/soil mixture, which has been shown to impart minor increases (<10%) to the CEC relative to soils with no biochar

added (Moradi & Karimi, 2020; Nguyen et al, 2018; Omara et al, 2023). Additionally, there are some practical matters that make CEC determinations less reliable or less meaningful and those are:

1. The pH of the environment can significantly impact the results of CEC measurements. In the lab, a neutral (pH 7) aqueous solution is used in CEC quantifications and does not reflect the variable pH levels found in real world environments.
2. High inorganic carbonate content in testing media can interfere with CEC measurements. All woods contain carbonates, primarily in the form of potassium carbonate.
3. Cations need to be able to diffuse into pores to be able to fully exchange with acidic protons on the surface of the media being tested. As most biochars contain significant amounts of micropores, many exchange sites are not able to be probed as slow diffusion rates into micropores and water's high surface tension prohibit reliable results.

3.2 Proximate, Ultimate and Inorganic Carbon Analysis

All 15 biochar products produced for this project (see list in Table 1.1) were sent out to an external analytical testing lab (Timber Products Inspection, Conyers, GA) for proximate, ultimate and inorganic carbon testing. All characterizations were performed in duplicate with the average value being reported. These tests are considered compositional analyses and provide the following information:

1. Proximate (weight percentages): Moisture, Volatile Matter, Fixed Carbon, and Ash
2. Ultimate Analysis (weight percentages): elemental C, H, N, O and S
3. Inorganic C (weight percentage): elemental C found in ash formed during proximate analysis

These characterizations provide critical insights into the physicochemical properties of the biochar products and into the success of controlling pyrolysis conditions during production runs. When organic biomass is subjected to heating in low oxygen environments thermal degradation will begin at ~250-300 °C in the hemicellulose fraction of the biomass, while temperatures of ~750 °C are required to ensure complete degradation of the lignin fraction of the material. During thermal degradation a plethora of reaction types take place including dehydration, depolymerization, decarboxylation, carbonization and many more. The volatile byproducts generated in these reactions contain a higher oxygen and hydrogen content and lower carbon content relative to their concentrations in the raw feedstock. This results in the following trends when comparing these data sets to the highest thermal treatment (HTT, aka maximum pyrolysis temperature) temperatures:

↑ HTT : ↑ Fixed Carbon
↑ HTT : ↑ Ash
↑ HTT : ↓ Volatile Matter
↑ HTT : ↑ %C
↑ HTT : ↓ %H
↑ HTT : ↓ %O

Many of these trends should start to plateau at temperatures above ~750 °C as increasing temperatures beyond this results in minimal further devolatilization and carbonization is closer to completion. Below

in Figure 3.1, the set of 10 biochar products produced under 100% N_2 have their proximate and ultimate analysis results plotted vs. HTT.

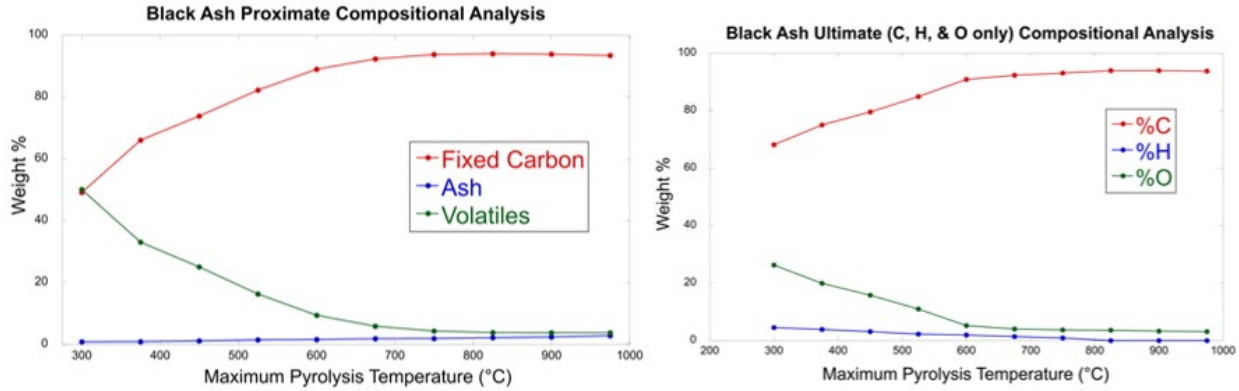

Figure 3.1 Plots of Proximate and Ultimate data vs. HTT for set of 10 biochar products produced under 100% N_2 sweep gas.

These plots are consistent with our expectations and are further evidence of tight temperature control during biochar production. The thermocouple probe that was placed down the center of the sample basket used to hold the biomass for biochar production runs had its values recorded throughout all biochar production runs. For all the runs using 100% N_2 as the sweep gas, the recorded temperatures stayed with in ±2 °C of the targeted HTT while samples produced with 4% O_2 in the sweep gas stayed within ±10 °C of the targeted HTT. Oxygen reacts exothermically with the carbon in the biomass and results in sample temperatures increasing slightly above the targeted HTT at certain times during the production run.

The ash generated as part of the proximate analysis was further analyzed by CHN combustion to determine the weight % of C found in the ash. The carbon in the ash is referred to as inorganic carbon as virtually all the carbon remaining in ash is due to the presence of inorganic carbonate minerals (e.g., K_2CO_3 or Na_2CO_3). As part of the ultimate analysis, the total C (organic plus inorganic) content is determined and to be able to calculate the organic carbon (total C – inorganic C = organic C) content, the inorganic carbon amount must be subtracted from the total. The organic C content is an important metric as it allows for the determination of the $H:C_{org}$ molar ratio. The $H:C_{org}$ ratio is a ubiquitous value used by biochar producers and researchers alike and is the primary property used to compare the relative stability of the C in the sample—and therefore is an indicator of its potential longevity for sequestering carbon. It is also used the value used to determine if the material can be considered "biochar."

The current definition that is widely used (e.g., by the World Biochar Certificate guidelines (EBC v. 10.4, 2024) states a sample must have a $H:C_{org}$ value of <0.7 to qualify. Lastly, there are a variety of types of biochar kilns used for production and many of them (e.g. flame cap kilns or large indirectly heated rotary kilns) do not have the ability to probe the HTT experienced by the biomass during production and so rather than qualifying a biochar product by its HTT (widespread practice), we prefer to use the $H:C_{org}$

value as an indicator of degree of carbonization instead of HTT. Following the trends outlined above, one should also expect that the $H:C_{org}$ should decrease as the HTT increases. This is due to H loss outpacing C loss as the HTT increases. When HTT values go above ~800 °C, there is an undetectable level of H remaining in our samples and so the $H:C_{org}$ values essentially go to zero. Figure 3.2 below, shows an overlay plot of $H:C_{org}$ vs. HTT for both the series of biochar products produced with 100% N_2 sweep gas, and the series of samples produced with 4% O_2 introduced in the sweep gas. The introduction of O_2 did not have an impact on the resulting $H:C_{org}$ values when compared to the 100% N_2 sweep gas samples.

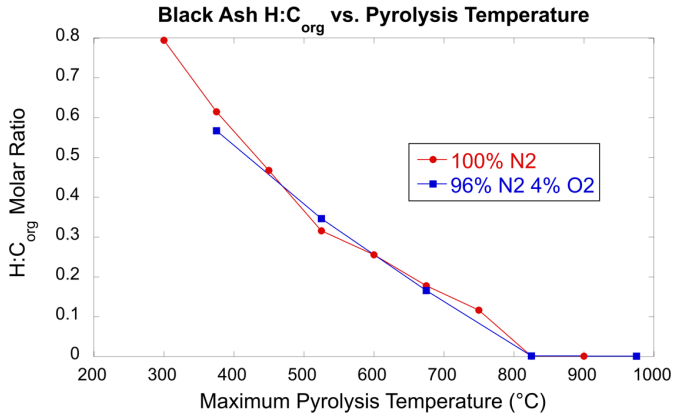

Figure 3.2 A plot of $H:C_{org}$ vs. HTT for samples produced under 100% N_2 (red) and under 96% N_2 and 4% O_2 (blue).

3.3 Extractives Quantification

Improper handling of generated volatile byproducts and inadequately long residence times at HTT are the most responsible mechanisms during biochar production runs which result in an unwanted amount of volatile organic material being deposited on the product surface. Buildup of wood tar on the exhaust ports (plugging) of biochar kilns can result in a buildup of gaseous organics in the pyrolysis chamber and these compounds can then redeposit on the biochar surface during cooling. Another way volatiles can build up on the surface is through short residence times, if one considers from the vantage of a volatile compound liberated in the core of a biomass particle during heating, that volatile compound has a long journey through the porous matrix of the biomass before it is truly liberated and separated from the biochar product. Insufficient residence times can then result in that liberated compound not being able to exit the particle and it will redeposit upon cooling.

Surface deposits of these organic materials on biochar products can result in the unintended leaching of pyrolysis byproducts into the environment and, even more critically, can occupy surface sites that could otherwise adsorb environmental contaminants in filtration applications, as is the case for this project. The presence of unacceptably high levels of volatile organics in biochar products is a very common issue and is why we quantify all biochar products used in our research efforts to ensure that the pyrolysis successfully separated the generated volatile organics from the biochar product.

To qualify a biochar production run as having adequately low volatile organic content, a Soxhlet extraction is performed using a 50/50 mixture of benzene (non-polar) and ethanol (polar). Since benzene (80 °C) and ethanol (78 °C) have very similar boiling points but much different polarities, they make for a good mixture for maximizing the extractives yield as some compounds found in volatile deposits are more soluble (more extractable) in polar solvents while others are more soluble in non-polar solvents. After 15 h of run time for the Soxhlet extraction, the resulting extractives solution has all the volatile solvent (benzene/ethanol) remaining removed via rotary evaporation. The mass of the collective extractives is measured, and the extractives content is reported as a weight % relative to the mass of starting material (g of extractives/g of starting material × 100). Having performed hundreds of these extractions, and in consultation with fellow biochar practitioners, we have determined that an extractives content of <0.25% by weight indicates adequate separation of generated volatile organics from a biochar product.

In Figure 3.3 below, a plot of extractives content vs. HTT is shown for the series of biochar products produced using a 100% N_2 sweep gas environment. It should be noted that we chose to test a wide range of HTTs (300-975 °C) for comparison purposes for this project, and the two products with the lowest HTTs (300 and 375 °C) had extractives content above the 0.25% threshold. The high values found in these two products is not an indication of improper handling of volatiles or of an inadequately long residence time, but rather a result of very low HTT conditions. For all subsequent sorption testing, the products with HTTs >375 °C should present zero complications, while the two lowest HTT products (300, 375) will undoubtedly be impacted by the high volatile organic content, particularly as leachates from those products will appear as dissolved organic carbon (DOC).

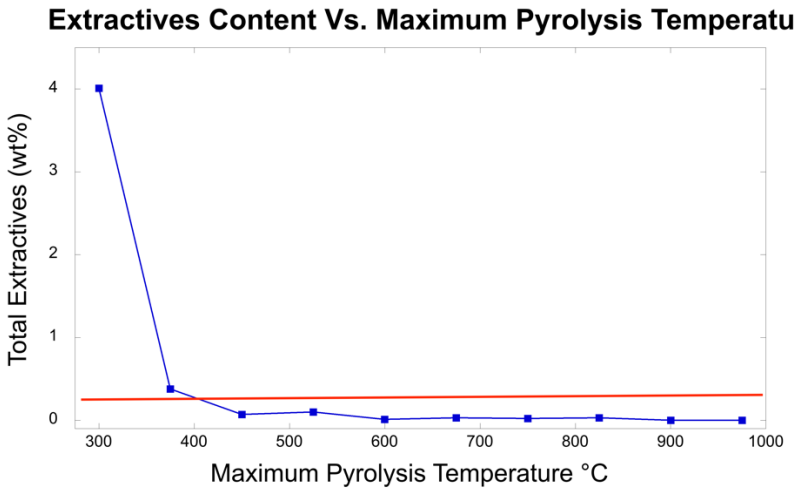

Figure 3.3 A plot of extractives content vs. HTT for the series of biochar products produced using a 100% N_2 sweep gas. Data points below the horizontal red line (at Y = 0.25%) represent samples with adequately low extractives content.

3.4 Complete Pore Size Distribution (PSD).

The surface morphology of a material encompasses a range various quantifiable metrics including specific surface area (SSA), total pore volume (TPV), %porosity, etc. Depending on the nature of the material being assessed, some measurements are not feasible. For example, biochar samples are inherently microporous, rendering the ubiquitous N_2-based BET SSA measurement unreliable (Thommes et al, 2015). The BET SSA method, when applicable, is a relatively fast, inexpensive measurement to perform and is widely used to compare the porosity of various materials to one another. Since this method is unavailable for biochar products, alternatives measurements must be used. The Chemistry & Materials Science lab at NRRI worked with the engineers at Micromeritics Inc. (manufacturer of the gas adsorption analyzer used here) to onboard a so-called "dual gas analysis" method which was detailed in a publication authored by the same engineers from Micromeritics (Jagiello et al, 2015). By combining data from gas adsorption isotherms of both CO_2 (273 K) and N_2 (77 K) and using two-dimensional non-local density functional theory (2D-NLDFT) to model the PSD, repeatable, reliable results for probing the PSD of microporous biochar products can be afforded. If combined with data from mercury intrusion porosimetry (MIP) experiments, one can produce a complete PSD for the material covering a pore range from 0.36 to 500,000 nm. Below are the pore ranges covered by the 3 separate experiments required to perform a complete PSD assessment:

1) CO_2 gas adsorption (0.36 to 1 nm)
2) N_2 gas adsorption (0.7 to 50 nm)
3) MIP (5 to 500,000 nm)

While the MIP instrument used for this project has the capability of probing pores sizes as large as 500,000 nm in diameter, the upper range is limited by the particle size of the material being assessed. For all of our MIP experiments, the biochar products were milled and sized to -10/+20 mesh, which means the smallest particles in any given sample should be no smaller than 840 microns (840,000 nm) in diameter. The recommendation is that PSD data should only be presented up to a value which is 25% of the diameter of the smallest particles in the sample, so for our experiments an upper limit to our PSD range would be 210 microns or 210,000 nm (840 × 0.25 = 210). The reason for this is that interparticle voids (gaps between particles) appear the same as intraparticle pores (pores in the particle) and when data reveals porosity in the upper range, those values must be excluded as they cannot be assigned to pores within the material. The use of the 25% conversion is modelled for perfectly spherical particles and if your particles deviate from that shape, the accessible range for presenting PSD data could be even smaller. This was the case for our samples, and experimentation revealed that the appearance of interparticle voids starting at pore diameters of 100,000 nm and above. For this reason, the functional working range of our complete PSD assessments is 0.36 to 100,000 nm.

For visualizing data from complete PSD experiments, the data is plotted with pore diameters (in nm) on a logarithmic x-axis and the Y-values can be presented as either *DV* (change in volume between neighboring data points), *DV/Dd* (change in Volume divided by change in pore diameter *d*), or as *DV/D* log *d* (change in volume divided by the log of the pore diameter *d*). The different options for treating the Y-values are there to give the presenter of the data options for visualization, the raw data is the

same regardless of which option is chosen (Liu & Ostadhassan, 2019). To "emphasize" (increase the relative Y-axis value) small diameter pores (<5 nm), choosing *DV/Dd* for Y-axis values will accomplish this, while to emphasize the larger pores (>100 nm), *DV/D* log *d* should be selected. Since our complete PSD experiments have a range of pore diameters from 036 to 100,000 nm, there isn't one choice for the treatment of Y-values that will emphasize pores across the entire range. Through consultation, again with the experts from Micromeritics Inc., it was decided that using *DV/D* log *d* for Y-axis values was the most appropriate. It is once more important to note that this decision does not impact the data reported, it is simply an esthetic choice for visualizing the entire complete PSD data set on a single plot.

In Figure 3.4a below, an example of a complete PSD overlayed with the cumulative pore volume (this is the raw data set used to calculate *DV*, *DV/Dd,* and *DV/D* log *d*) is presented. The cumulative pore volume data set can also be used to calculate the total pore volume within any range of pore diameters. We created a spreadsheet tool which performs a linear interpolation between neighboring cumulative pore volume data points, which allows users to define an upper and lower end to their pore range of interest. We refer to this as a user-defined, regime-specific TPV (UDRS-TPV) calculation. TPV values for different ranges of pore diameters can be presented as bar graphs (see Figure 3.4b) and can be a nice alternative to looking at complete PSD plots as they are far less busy and make for easy comparisons of UDRS-TPVs between biochar products. Referring to Figure 3.4a, the UDRS-TPV ranges we have chosen to use for comparisons are as follows:

A) 0.36 to 1.3 nm ultramicroporous (uMicP)
B) 1.3 to 50 nm *pseudo*-mesoporous (*p*MesP)
C) 50 to 3,000 nm vascular pores (vP)
D) 3,000 to 100, 000 *pseudo*-macroporous (*p*MacP)
E) >100,000 nm interparticle pores, data not considered

When looking at Figure 4a (or Figure X), one can visualize why we chose these particular ranges to calculate TPVs from as they represent distinctive regions of porosity.

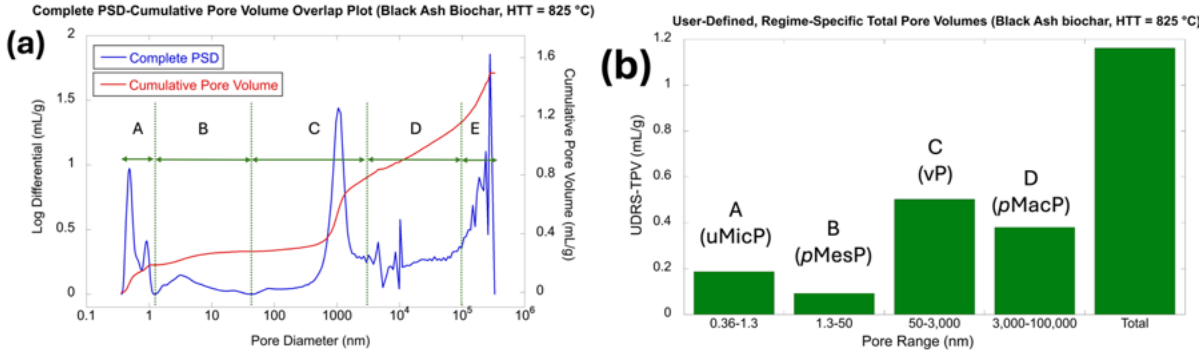

Figure 3.4 a) A complete PSD and cumulative pore volume overlay plot of black ash biochar produced at an HTT of 825 °C and under 100% N_2 sweep gas. b) A graph comparing TPVs within pore ranges outline above for regions A-D.

The PSD plots for the complete (10 products) set of samples produced under 100% N_2 sweep gas conditions can be seen in Figure 3.5a. In figure 3.5b, the TPVs within each of our defined pore volume regimes (uMicP, *p*MesP, vP, & *p*MacP) has been graphed, making for easy comparisons on the TPV within each regime. The general trends show that the TPV in the uMicP regime steadily increases with increasing HTT, with the TPV approximately doubling as the temperature goes from the lowest pyrolysis conditions (300 °C) to the highest (975 °C). In the *p*MesP regime, there is not a clear trend with HTT, but it does appear that moderate pyrolysis conditions (450-600 °C) produce the largest pore volumes in this regime. We do not have definitive evidence for why this pore volume regime does not produce a clearer trend, but it is possible that the stability of these pore sizes is impacted by HTT and high temperatures could cause these pores to collapse. As in the uMicP regime, the vP TPVs show a clear trend of increasing in total volume as the HTT increases, resulting in an approximate 35% increase in pore volume going from the low HTT (300 °C) to the high end (975 °C). This regime was given the descriptor of "vascular pores" and they are present due to the cell walls found in the xylem acting as templates for carbonization. In other words, the initial morphology of the raw biomass is reflected in the morphology of the biochar produced from it. This templating mechanism is what affords such highly porous materials upon conversion to biochar. Two scanning electron microscopy (SEM) images are presented in Figure 3.6, allowing for the clear visualization of the vascular pores, and are consistent with the presence of significant TPV in the vP range of our PSD experiments. The TPVs found in the *p*MacP regime shows no evidence of dependence on HTT and have nearly consistent TPVs across the HTT range.

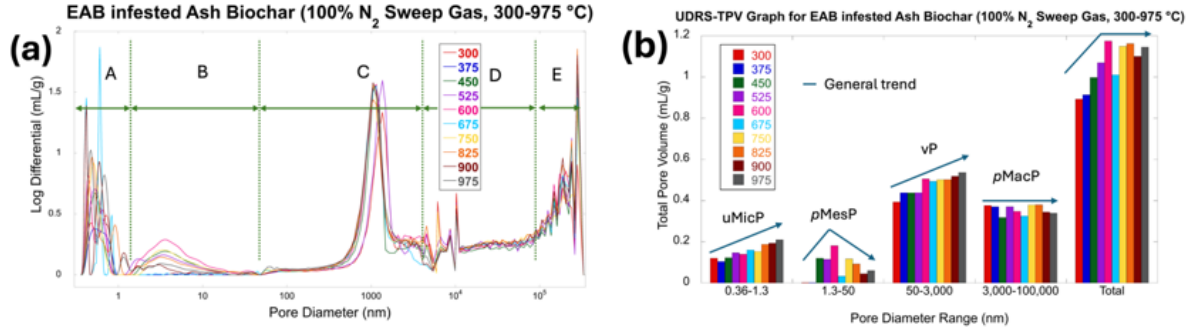

Figure 3.5 a) A complete PSD overlay plot of all samples produced with 100% N_2 sweep gas. b) UDRS-TPV bar graph showing the TPV within each of the four designated pore volume regimes and the combined TPV ("Total") for the same set of products as descried in a).

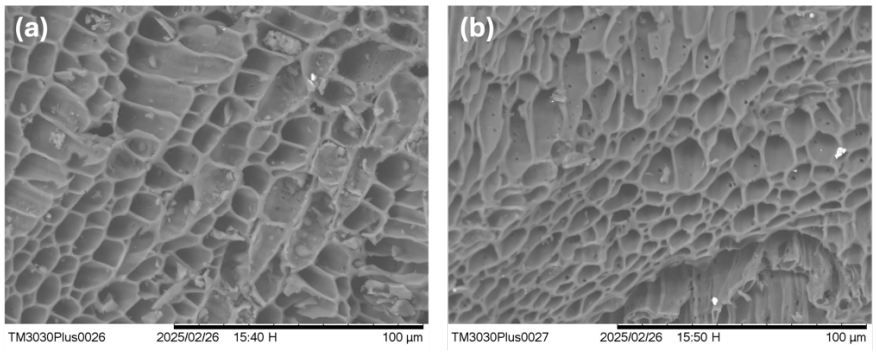

Figure 3.6 Scanning electron microscopy (SEM) images of a) black ash biochar HTT = 525 °C and b) black ash biochar HTT = 825 °C both at 1000X magnification.

A second set of biochar products was produced using an alternative sweep gas. For this set of 5 products, the sweep gas was changed from 100% N_2 to a mixture of 96% N_2 and 4% O_2. These products were produced at HTTs of 375, 525, 675, 825 and 975 °C. The introduction of O_2 was intended to "activate" the biochar samples. Activation occurs when an employed activating agent reacts with the surface of a carbon-based material, in our case the surface of the biochar. As a carbon surface deviates from being planar or flat, its reactivity increases due to the relatively instability of the surface atoms. This results in the smallest pore surfaces having the highest reactivity and therefore react first with an introduced activating reagent. In the case of the biochar products produced here, activation should result in the widening of its smallest pores via combustion with introduced O_2 and should be reflected in the complete PSD experiments. Previous efforts in our labs, clearly showed the efficacy of activating biochar samples by introducing 4% O_2 into the sweep gas (See Figure 1.1). In this plot, the disappearance of porosity in pore ranges <0.9 nm and an increase porosity in the range of 0.9 to 1.5 nm is observed upon introduction of O_2 in the sweep gas. These results were anticipated and clearly demonstrated the efficacy of oxygen as an activating agent, widening the pores with diameters <0.9 nm.

The reason these 5 activation experiments were undertaken was to impart changes to the PSD relative to the samples produced under 100% N_2 with the hopes that these changes in PSD would impact their sorption performance properties. By making comparisons of UDRS-TPVs with various sorption performance values (e.g., Cu^{2+} sorption), we hoped to find a correlation between the PSD of the product and its sorption performance. In the context of this project, an engineer may be looking to use a commercial biochar product as a component of an engineered soil mixture for a roadside swale bioretention system (BRS) and may not have much knowledge about the physicochemical nature of the biochar on hand. Since biochar products on the market come from many different feedstocks and are produced under varying pyrolysis conditions, a wide variety of PSDs would be anticipated when comparing various commercial materials. Were a strong dependency observed between a particular UDRS-TPV and sorption performance; a complete PSD experiment would allow a biochar end-user to determine if a particular biochar product was suitable for their application.

Unfortunately, the 5 biochar products produced here under 4% O_2, when compared to their 100% N_2 counterparts (same HTT), did not produce the anticipated results as we saw for experiments shown in Figure 1.1. Had these experiments gone as anticipated, two clear observations would have been seen

when comparing analogous runs of 100% N_2 sweep gas with runs performed under 4% O_2; those being a significant decrease, or complete disappearance, of pores in the uMicP region and a significant increase in the TPV in the *p*MesP region. Virtually no changes were observed in the uMicP region and unpredictable and minor changes were observed in the *p*MesP region. In Figure 3.7 below, 3 complete PSD plots are presented overlaying the 100% N_2 results with the 4% O_2. When comparing analog pairs produced at HTTs of 675 °C, the *p*MesP TPV increased (Δ = +284%) upon introduction of O_2, while in the 525 °C pair the *p*MesP TPV decreased (Δ = -182%), and lastly in the 375 °C pair the TPV in the *p*MesP range was virtually unchanged. These observations were disappointing, and the conclusion must be drawn that these samples do not present us with the variation in PSD that we were hoping to produce.

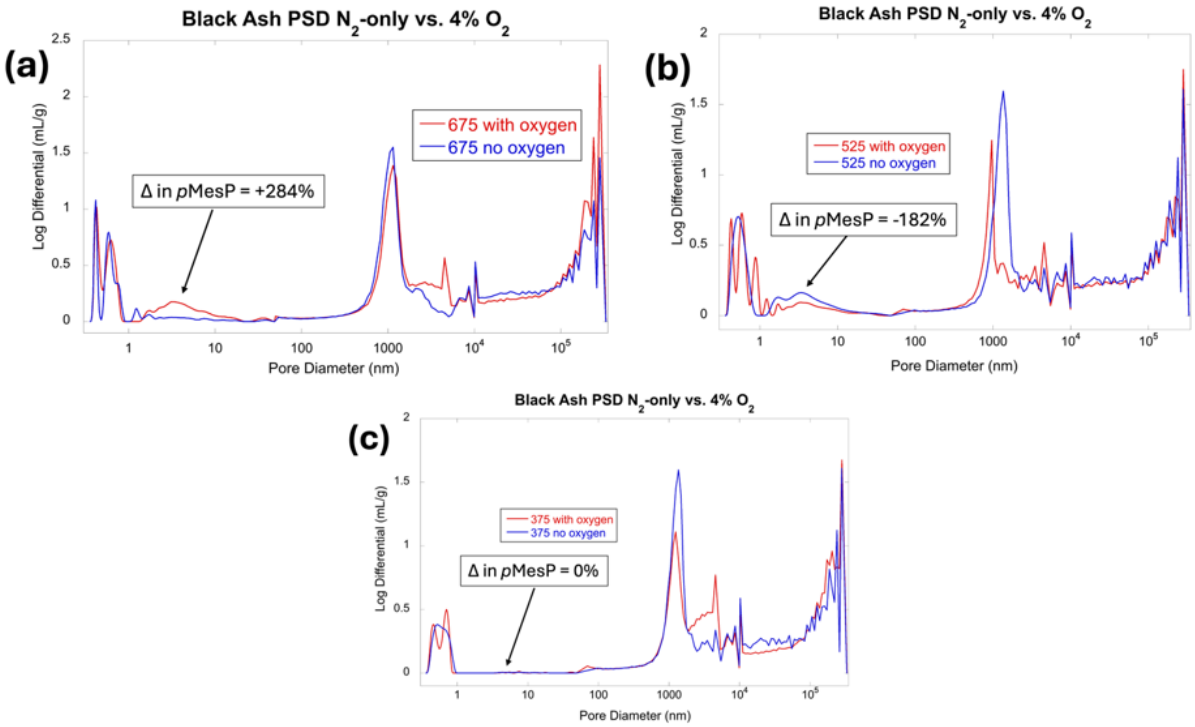

Figure 3.7 Overlay plots for complete PSD comparing analogous products produced with a 100% N_2 sweep gas (blue) and with 96% N_2/4% O_2 (red) for samples produced at HTTs of a) 675 °C, b) 525 °C, and c) 375 °C.

3.5 Water Holding Capacity

Since trees need the ability to transport water from their roots to their leaves, they have evolved vascular networks (vessel elements in hardwoods, tracheids in softwoods) to accomplish this. The highly porous nature, typical of all unmodified woody biochar products, can be attributed to the retained, vascular morphology from the raw biomass upon conversion to biochar. This retention of morphology results in biochar having right-sized pores for water uptake and woody biochar products tend to have WHCs of values between 2 and 6. To determine WHCs, a recorded weight (~2 g) of biochar milled to a set size (in our case -10/+20 mesh) is loaded into a Falcon tube with 50 mL of DI water and agitated on

an orbital shaker for 2 hours. After 2 hours, the biochar product is transferred to a gravity filtration set up and the wet biochar is allowed to filter off unsorbed water for 30 min. prior to removing and weighing the wet biochar sample. The WHC is calculated as follows and reports the g of sorbed water per g of dry biochar:

$$WHC = \frac{\text{g of WBC} - \text{g of DBC}}{\text{g of DBC}}$$ where WBC = wetted biochar and DBC = dry biochar

The value of determining WHC for biochar products is that it is an inexpensive, cheap experiment that anyone could perform without the need for expensive instrumentation or equipment and allows for qualification of the product has having suitable porosity for sorption-based applications. In Figure 3.8, the WHC values for all biochar products produced under a 100% N_2 sweep gas are presented. These values in this figure represent the average from a set of triplicate experiments. For this series of products, the WHC is clearly independent of HTT as all products in this series had similar values ranging from 3.27 to 3.90 ($g_{sorbed\ water}/g_{biochar}$). This is not surprising as PSD results revealed the presence of significant vascular pore (vP) volumes across the entire HTT range. While the vP volumes do show a trend of increasing with HTT, it is not completely surprising that the WHC values do not correlate directly with these increases as the surface chemistry, and therefore relative hydrophobicity, changes with HTT as well. While the increasing vP volumes are increasing with HTT and should result in higher WHCs, the hydrophobicity should also increase with HTT which could counteract any WHC gains made from increased vP volume.

In contrast, carbon-based materials without vascular pores (e.g., coal and coke products) consistently show lower WHCs when compared to their more porous woody biochar counterparts. A set of 3 "unactivated" coke samples (anode coke, breeze coke and foundry coke) were obtained along with a set of 3 activated carbons and the WHC values of these products were measured as comparisons to our biochar products. The unactivated coke samples produced values ranging from 0.32 to 0.71, while the activated samples showed WHCs in the range of 0.91 to 1.76. We have performed PSD experiments on all these additional samples (coke products and activated carbon products) as well and have confirmed that they have virtually no or significantly less (coconut AC) TPV in the vP regime. For the set of 10 biochar samples produced under 100% N_2 sweep gas, the vP TPVs ranged from 0.394 to 0.537 mL/g (see Figure 3.5b), while the coconut AC had a vP TPV of 0.172 mL/g and the rest of the comparison carbons (all cokes, bitumen AC, and coal AC) had vP TPVs < 0.0942 mL/g.

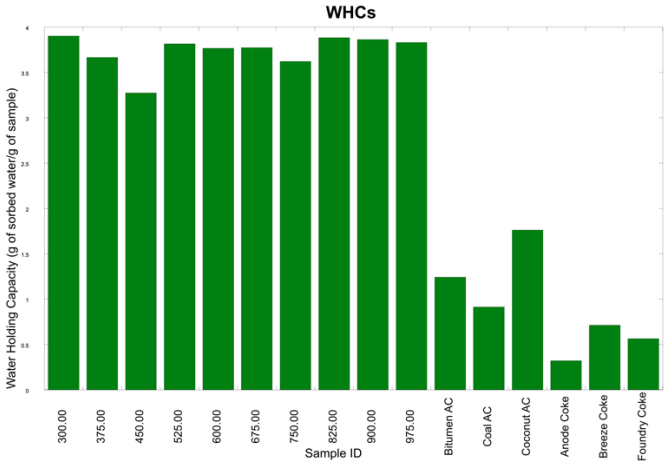

Figure 3.8 Bar graph of measured WHCs for the set of biochar products produced under 100% N_2 sweep gas (300-975 °C), a series of 3 activated carbons (AC), and a series of 3 "unactivated" coke products.

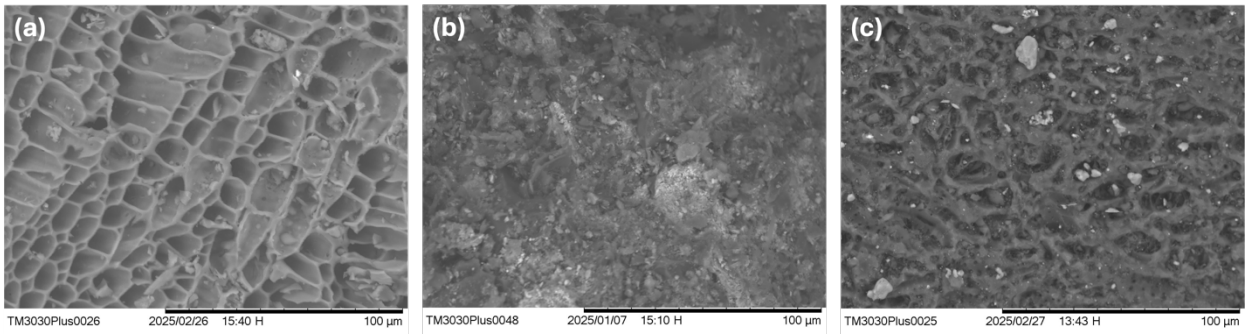

Figure 3.9 Scanning electron microscopy (SEM) images of various carbon-based materials all at 1000X magnification: a) black ash biochar HTT = 525 °C, b) breeze coke, and c) coconut activated carbon.

These observations are consistent with WHC experiments being predictive for the presence of vascular pores and are further corroborated by SEM images clearly showing a lack of vascular pores. In Figure 3.9, SEM images of a) one of our biochar products (HTT = 525 °C, sweep gas = 100% N_2), b) an unactivated carbon (breeze coke), and c) an activated carbon (coconut AC) are juxtaposed to show the differences in porosity. The sorption performance of biochar products, particularly when they have low *p*MesP (most cases), require the presence of vascular pores to produce targeted performance results. This case will be laid out in more detail in the sections to come, but the conclusion from these WHC experiments is that this test can be used to probe for the presence of vascular pores and should result in a value ≥ 3.00 ($g_{sorbed\ water}/g_{biochar}$).

3.6 Butane Activity

As part of our workplan, we hoped to produce a series of 5 activated biochar samples by introducing 4% O_2 into the sweep gas, with the hopes that we could significantly increase the TPV in the *p*MesP range relative to samples produced under 100% N_2. This was targeted to increase variety in PSDs between tested biochar products to try and gain insight into how differences in the *p*MesP might impact their

sorption performance towards selected environmental contaminants of concern. While performing a complete PSD analysis of a biochar material will certainly provide one with a quantification of the *p*MesP TPV, it is a very expensive test not practical for most biochar practitioners, and so butane activity (fast and cheap) was selected as an alternative proxy test for comparing mesoporosities (or *p*MesP).

Butane has a kinetic diameter of 0.47 nm and has been shown to have increased absorption in materials when the TPV is increased in the pore range of 2.8-3.8 nm (Lee et al, 2021). This is logical considering the sorption method for hydrocarbons (e.g., butane) on biochars is what is called adsorptive pore-filling (Nguyen et al, 2007). Pore-filling requires that adsorbents become "trapped" in pores and is less reliant on electrostatic interactions between the substrate and the adsorbent. The ratio of the adsorbent molecule diameter (0.47 nm for butane) to the pore diameter can be optimized for pore-filling adsorption when the pore diameter is ~5-10X that of the adsorbent. The previously cited paper (ibid) revealed that a range of 2.8-3.8 nm was optimal for butane pore-filling, reflecting a pore diameter: adsorbent diameter ratio range of 5.96 (2.8/0.47) to 8.09 (3.8/0.47). Looking at pore diameters resulting in ratios < 5 or >10 (outside of optimal 5-10X range), the quantity of adsorbent trapped via pore filling goes down. This pore-filling mechanism is what is utilized to perform gas adsorption experiments (e.g., N_2 BET SSA) and is why gas adsorption experiments only allow for probing a relatively small range of pores. Larger pores (> 50 nm) cannot be probed as those larger pores result in ratios significantly outside the 5-10X range and adsorbents can no longer be trapped.

As described previously, our attempts at significantly increasing the *p*MesP TPV by introducing oxygen in the sweep gas as an activating agent were not successful. Because of this fact, the results from our butane activities are not very useful (see Figure 3.10) and showed no dependency on HTT or on O_2 activation, which again, is not surprising considering we do not see any trends between *p*MesP TPV and HTT. The measured butane activities for the bitumen AC, the coconut AC, and coal AC were 23.293, 33.323, and 23.024 g of adsorbed butane/ 100 g of sample respectively. The butane activity values for our biochar products ranged from 0.87 to 7.67 g of adsorbed butane/ 100 g of sample, which is consistent with the much lower porosity in the *p*MesP regime (see Figure 3.11b). It should also be pointed out that in Figure 3.11a, it is very easy to see the lack of vascular pores in AC samples compared to our biochar products—this will come up again later in the discussion. The takeaway from this section is that butane activity is very useful for probing for the presence of mesoporosity, but most biochar products being produced commercially do not undergo activation and have significantly lower TPVs in the *p*MesP regime when compared to commercial AC products.

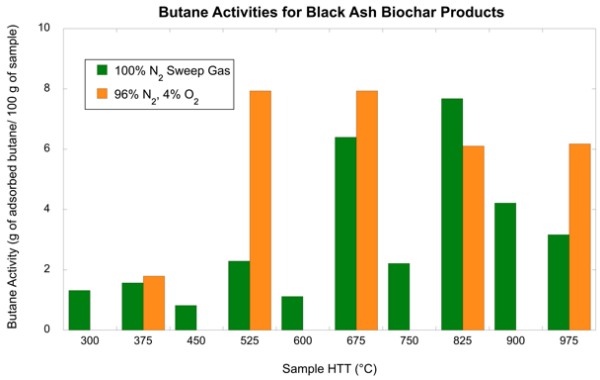

Figure 3.10 Bar graph of Butane Activities for biochar products produced with 100% N_2 sweep gas (green) and with a 96% N_2/4% O_2 sweep gas (orange).

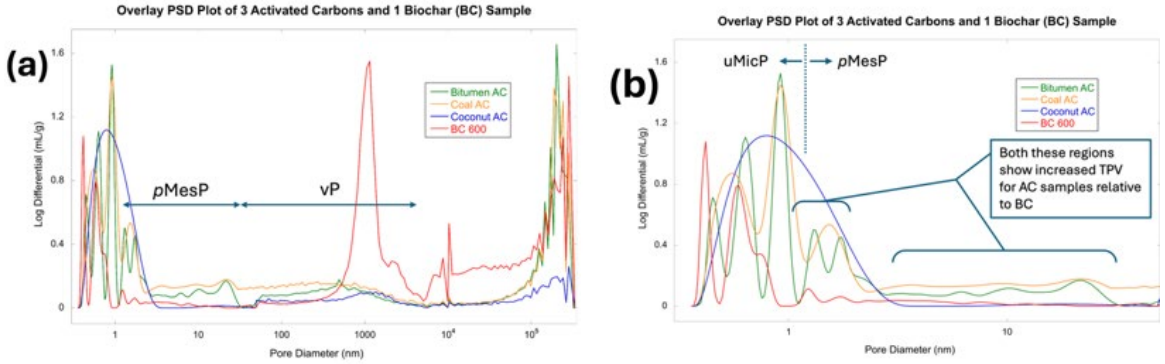

Figure 3.11 Overlay PSD plots for 3 activated carbon (AC) samples and the biochar (BC) product produced at 600 °C under 100% N_2 sweep gas. a) full pore diameter range (0.36 to 350,000 nm), b) small pore diameter range (0.36 to 50 nm).

3.7 Coke Reactivity Index and SEM

In further efforts to test carbon-based materials with markedly different PSDs compared to the black ash biochar samples, two activated carbon samples (bituminous AC & coconut AC) along with a coal product (breeze coke) were explored. The differences in PSDs in these three non-biochar, carbon-based materials is apparent when looking at both the complete PSD plots and the UDRS-TPV bar graphs seen in Figure 3.12. The breeze coke sample was chosen to represent a carbon-based material with the least porosity, and this was confirmed as the measured pore volumes in each of the pore diameter ranges was significantly lower compared to all other materials. It should be noted that, while care was taken to size all of these products similarly (-10/+20 mesh), the breeze cokes interparticle voids started to appear at a lower point (40,000 nm) when compared to the other samples (100,000 nm). As these voids need to be discounted when determining pore volumes, the *p*MacP and Total pore volume ranges used for breeze coke were 3,000 – 40,000 nm and 0.36 to 40,000 nm respectively. This result is likely due to significantly different particle shapes in breeze coke when compared to the other 3 materials.

The two activated carbon samples were selected to offer materials with increased mesoporosity when compared to the biochar sample, and this was confirmed when looking at the measured TPV values for the *p*MesP range (see Figure 3.12b), with the coconut AC and bituminous AC having 48% and 93% more pore volume respectively when compared to the biochar sample. The other major difference between the biochar sample and the other 3 carbon-based materials is the lack of vascular porosity, which is clearly evident from the data shown in Figure 3.12. Additionally, scanning electron microscope images (see Figure 3.13) of each of the 4 samples were collected and clearly reveal the major morphological differences between these materials, with the most stark difference coming when looking at the biochar image (Figure 3.13d), which clearly reveals the retained vascular structure. When collecting complete PSD data for samples is not feasible (lengthy and expensive test), SEM, while not quantitative, offers a quick, cheap alternative to verify the presence of vascular pores.

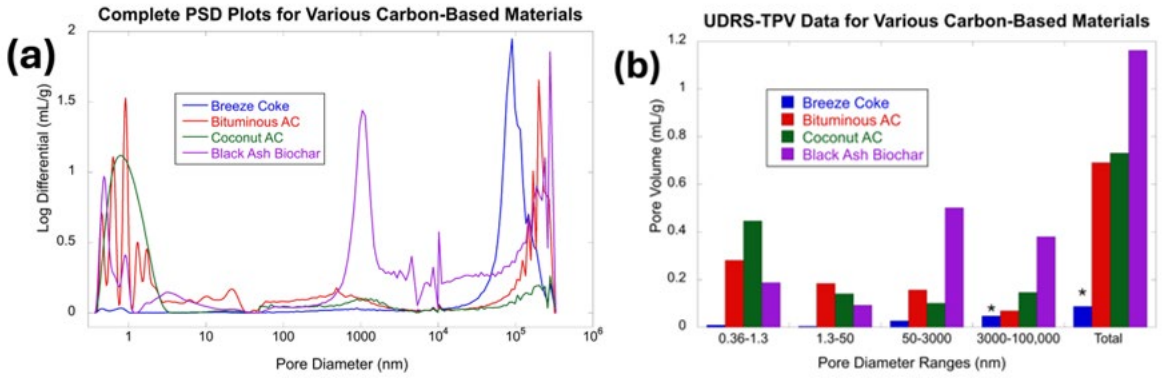

Figure 3.12 a) A complete PSD overlay plot for 4 carbon-based materials. b) User-defined, regime-specific TPV bar graph for the same 4 carbon-based materials. *The starred breeze coke pore ranges used were 3,000-40,000 for the *p*MacP range and the Total pore range used was 0.36 to 40,000 nm (explanation in narrative).

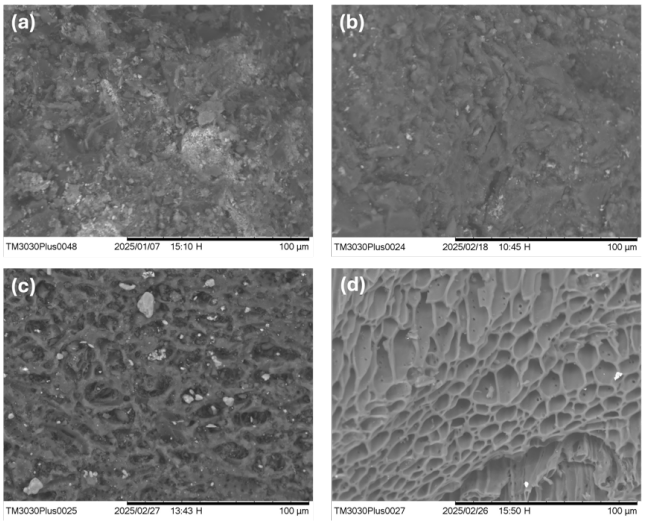

Figure 3.13 Scanning electron microscopy (SEM) images of a) breeze coke, b) bituminous AC, c) coconut AC, and d) black ash biochar all at 1000X magnification.

For adsorption-based experiments looking to gain insight into material morphology (e.g., N_2 BET SSA and butane activity), the results are impacted not only by the material's PSD, but also the material's surface chemistry. Furthermore, in many gas adsorption experiments, the samples must be cooled to afford adsorption of the gas (N_2: -196 °C, CO_2: 0 °C) and this often results in very long experiment times (several days often) due to the very slow diffusion rate of gases into small pores, which are abundant in biochar products. To explore alternative options, we decided that rather than relying on surface adsorption of a gas, we would use a reactive gas which would react at the surface of the material and by comparing the rate of weight loss, we could correlate that with material porosity (in this case the total pore volume).

This idea came about when, for another project, we were exploring the reactivity of various coke products used for steelmaking. The various flavors of coke had different porosities and therefore different reactivity rates as determined by a standard test called the coke reactivity index (CRI). In these experiments, a carbon-based material is heated to 1100 °C under inert gas before switching the heating chamber to a CO_2 gas environment. The sample weight is monitored over the two-hour duration the sample is exposed to CO_2 at 1100 °C and the % in weight loss is used to calculate the CRI (CRI = 100-%weight remaining at t= 2 hours). The reaction occurring in this experiment is known as the reverse-Boudouard reaction, where carbon from the sample reacts with CO_2, emitting two equivalents of carbon monoxide (CO), resulting in sample weight loss:

$$C_{sample} + CO_{2(g)} \rightarrow 2\ CO_{(g)}$$

This is an attractive test for three main reasons: 1) while surface chemistry impacts adsorption, it will have minimal effects on reactivity with CO_2, and therefore CRI is agnostic to surface chemistry differences, 2) The elevated temperature of 1100 °C alleviates concerns with diffusion times of the reactive gas into small pores, and 3) when compared to gas adsorption experiments, the experiment time for CRI is only a few hours compared to several days for gas adsorption experiments. In figure 3.14 below, the weight loss data for the 4 selected carbon-based materials is shown and produced CRI values of 13.50%, 21.89%, 28.46% and 48.61% respectively for the breeze coke, bituminous AC, coconut AC, and black ash biochar respectively. When comparing the CRI values to the total pore values (determined in our complete PSD analysis) a clear trend is observed where an increase in total pore volume results in an increase in CRI. In Figure 3.15, the plot of CRI vs. total pore volume is shown and this set of data resulted in a Pearson's r correlation coefficient of 0.932, a very strong correlation. We believe that CRI testing can offer an alternative method for probing the porosity of a carbon-based material when complete PSD efforts cannot be made, and we believe this to be a far superior test to butane activity. Future work will look to build upon this initial set of 4 samples to offer strengthened evidence for the use of CRI as a porosity-probing method, and while not proposed as part of Phase 2, we hope to have the capacity to expand this work there.

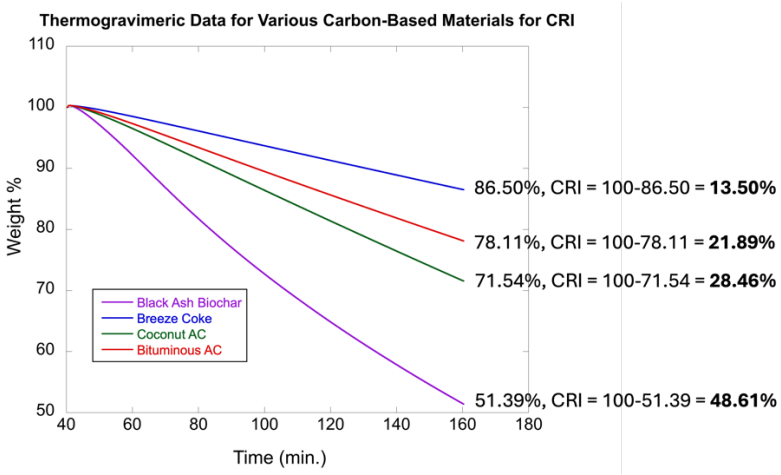

Figure 3.14 Thermogravimetric data collected for 4 carbon-based materials as part of CRI determinations.

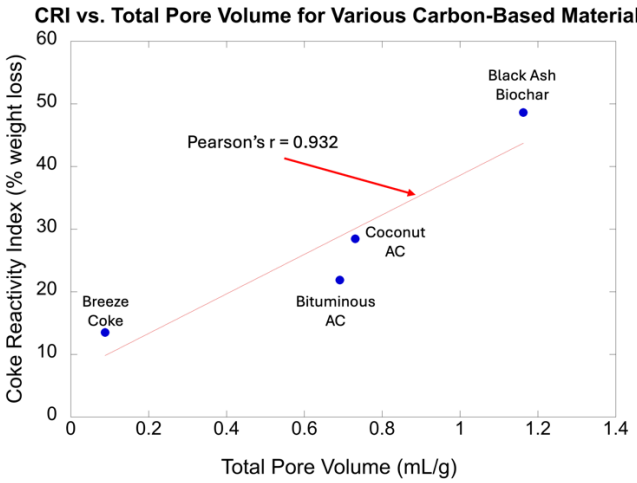

Figure 3.15 A plot of the coke reactivity index vs. the total pore volume for various carbon-based materials.

Chapter 4: Contaminant Sorption Performance and Statistical Evaluations.

4.1 Preliminary Leaching Tests.

Whenever a material is going to be assessed for its sorption performance, it is first necessary to understand what chemicals may be leached from the material under the conditions it is intended to be deployed. This is important to a) assure the material you are deploying does not itself, present contamination concerns and b) to ensure the material has a clean surface (exemplified by low leachate levels) for sorption of environmental contaminants. In the case of this project, where we will be looking to treat stormwater runoff from roadways, the preliminary leaching test condition required to assess is exposure to water. As such, preliminary tests for all biochar products examined here are first extracted with deionized (DI) water and the resulting aqueous solution is assessed for dissolved organic carbon (DOC) content via UV-Vis spectroscopy and phosphate (PO_4^{3-}) content via ion chromatography.

Since hydrocarbon (motor oil primarily) runoff from roadways is one of the contaminants we are looking to remediate by incorporating biochar into roadside swale BRSs, we have chosen to look at humic acid uptake as part of our batch sorption experiments (see section 4.2). Humic acid is a byproduct of biomass decomposition and is not a single type of molecule but rather encompasses a complex mixture of organic molecules. Humic acid is routinely used as a DOC surrogate in sorption-based experiments as these organic compounds are known to be soluble in water (necessity for aqueous sorption experiments) and there are rigorously characterized standard humic acid reagents available from the International Humic Substances Society (IHSS).

Any DOC released from these preliminary leaching tests can impact subsequent batch sorption results and quantifying the DOC content in biochar leachates is the primary driver for performing these preliminary leaching tests. In section 3.3, data was presented revealing that the two low temperature biochar products (HTTs of 300 and 375 °C) had significant levels of organic-solvent extractable material and this was also the case for the DI water extractions and in Figure 4.1 below, one can see that these two samples also had the highest DOC release. The impacts of extractable DOC present in biochar products in their sorption performance towards environmental DOC is presented in section 4.2 below.

Once the biochar products have been extracted with DI water, the resulting solution can be used not only to test for DOC, but also for assessing dissolved anions with minimal extra effort. While biochar does not present a significant risk of releasing high levels of unwanted nutrients into the environment (e.g., phosphate or nitrate), it is still worth looking at to confirm that the material being tested does not represent a significant source of unwanted nutrient release as the species can lead to the eutrophication of watersheds. For this project we chose to look at PO_4^{3-} release as an ancillary experiment and we were able to confirm that the biochar products produced here did not represent a significant source of PO_4^{3-} with ranges of 0.1 to 1.8 ppm (mg/kg of biochar) found in tested samples (See Figure 4.2). To provide some context, the design criteria for BRSs published by the MPCA suggests for soils used should be low

in phosphorus and suggests a range between 12 and 36 ppm, far exceeding the values seen in our biochar products.

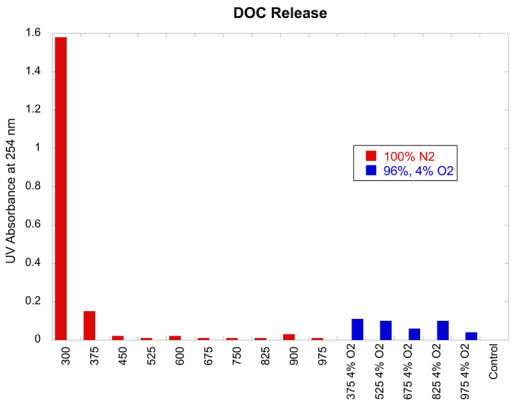

Figure 4.1 A bar graph of the UV absorbance of aqueous extractions of biochar with the products produced under 100% N_2 sweep gas conditions shown in red and the products produced under 96% N_2/4% O_2 shown in blue. The control shown here is DI water.

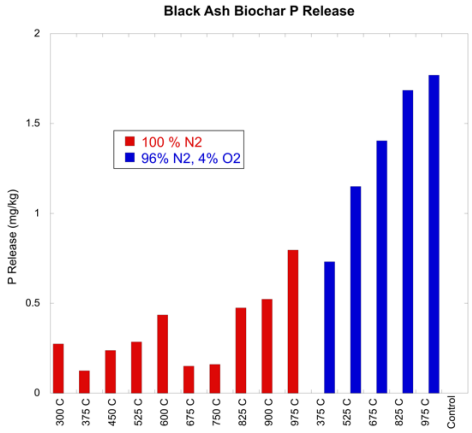

Figure 4.2 A bar graph of the phosphate released from biochars via aqueous extraction where products produced under 100% N_2 sweep gas conditions shown in red and the products produced under 96% N_2/4% O_2 shown in blue. The control shown here is DI water.

4.2 Biochar Batch Sorption Tests

All 15 biochar products produced for this project (See Table 1.1) were evaluated via batch sorption tests for their ability to uptake various contaminants of concern specific to stormwater roadway runoff. The contaminants chosen for evaluation were four metals (Cu, Ni, Zn, and Pb, all as +2 cations from metal salts) and humic acid (surrogate for DOC). In these experiments, 0.2 g of biochar product (sized to -60/+270 mesh) was loaded into a Falcon tube along with 50 mL of synthetic stormwater which had been spiked with the 5 contaminants (4 metals plus humic acid). This mixture was agitated on an orbital shaker for 24h before the tubes were both centrifuged and filtered (0.45 µm nylon filter) to separate the

biochar from the supernatant. The resulting aqueous supernatant was evaluated for metal content via inductively-coupled plasma-mass spectrometry (ICP-MS) and for DOC content via UV-Vis spectroscopy.

The initial concentrations of all five contaminants prior to mixing with biochar was known, and the difference in concentration after mixing with biochar and separation (centrifugation/filtration) was determined allowing for the quantification of sorption performance. There are two common ways the sorption performance in batch sorption experiments are presented. The first is referred to as normalized concentration (*N*) and simply reports the ratio of equilibrium contaminant concentration (C_e, concentration after separation from biochar) to initial contaminant concentration (C_0). The second representation of performance is referred to as K_d (K is the common symbol for equilibrium constant and d is a descriptor for "distribution"), also known as the partitioning or distribution coefficient. K_d values use the ratio of the change in contaminant concentration ($C_0 - C_e$) to the equilibrium concentration (C_e). That ratio is then converted to ppm (mg/kg) using the weight of the biochar sample using the conversion factor of (V/m) where V is the volume of solution used (50 mL in our case) and m is the mass of the biochar sample (~0.2 g in our case):

$$N = \frac{C_e}{C_0}$$

$$K_d = \frac{(C_0 - C_e)(\frac{V}{m})}{C_e}$$

When looking at these two equations, one will notice that for normalized concentration the initial concentration (C_0) is in the denominator while for K_d, the equilibrium concentration is in the numerator. This results in *N* values going down as sorption performance improves and K_d increasing as performance improves. Furthermore, K_d values are most typically plotted as Y-values on a logarithmic scale. The log values are used for visualization purposes as often one will want to compare performance values of materials with vastly different K_d values and without using a log scale, various values become dwarfed by neighboring values.

We will present the normalized concentration bar graphs of our data here, while the data presented in terms of log K_d can be seen in Appendix C. A bar graph plotting *N* values for the set of 10 biochar samples produced under 100% N_2 sweep gas conditions towards metal uptake can be seen in Figure 4.3. The controls chosen for comparison were two commercially available carbon materials. The "commercial biochar" is a biochar produced from southern yellow pine by the American Biochar Company, while the "activated carbon" is produced from bituminous coal (Calgon F400). For all metals (Cu, Ni, Zn and Pb) it is clear that the performance improves (decrease in *N*) for the materials produced at higher HTTs. In Figure 4.4, four graphs are shown for the individual metals, and a vertical, dashed cutoff line has been added to highlight that significant improvements in performance are seen as the HTT goes from 525 to 600 °C. The absolute % change in *N* values between HTTs of 525 and 600 °C are 88%, 57%, and 83% for Cu, Ni and Zn respectively. The Pb equilibrium concentrations, where HTT ≥ 600

°C, were shown to be below the instrument detection limits and so a % change in *N* cannot be presented. An example calculation for absolute % change in *N* for Cu is as follows:

$$Absolute\ \%\ Change\ in\ N = \frac{(C_{525} - C_{600})}{C_{525}} \times 100$$

$$Abs.\%\ Change\ N\ (Cu) = \frac{(0.17-0.02)}{0.17} \times 100 = 88\%$$

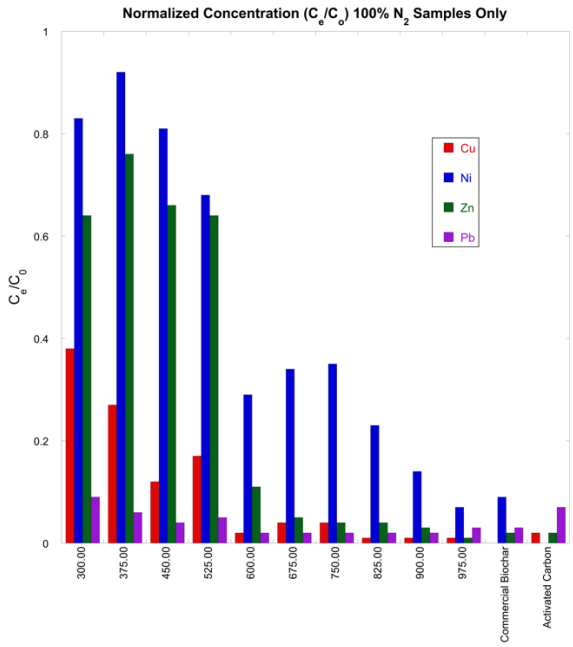

Figure 4.3 Bar graph plot for the normalized concentration values produced for batch sorption tests for 4 contaminant metals (Cu = red, Ni = blue, Zn = green, Pb = purple) using biochars produced under 100% N_2 sweep gas.

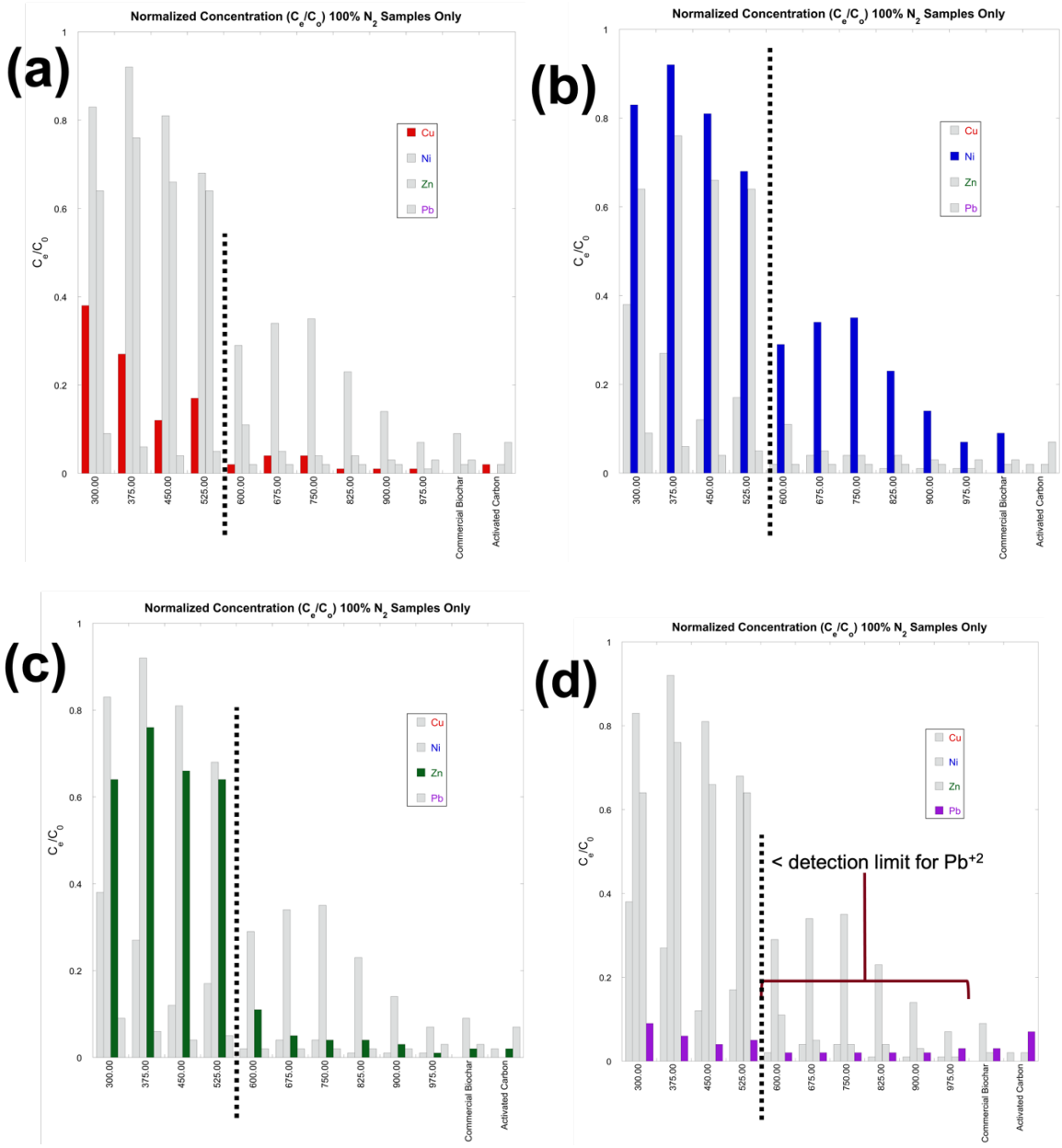

Figure 4.4 Bar graph plots for normalized concentrations highlighting sorption performance towards Cu (a), Ni (b), Zn (c), and Pb (d).

When comparing sorption performance of the biochars produced between 600 and 975 °C (values to the right of vertical dashed cutoff line) to the activated carbon performance for Cu, the average *N* (C_e/C_0) for these samples is 0.02166 compared to 0.0200 for activated carbon, indicating very similar performance. For Ni, the activated carbon performed better removing Ni below the detection limit and therefore no direct comparison of values is possible. For Zn, the average of the *N* values (HTT ≥ 600 °C) is 0.0467 compared to 0.0200 for activated carbon, showing slightly better performance for activated carbon, but the difference is rather insignificant. For Pb, the biochars actually outperformed activated carbon,

removing the Pb to below the detection limits, while the activate carbon sample still had detectable levels for Pb present at equilibrium.

As the introduction of O_2 in the sweep gas did not impart the significant difference in PSD that we were expecting, it is not surprising that a clear pattern did not arise when comparing sorption performance of samples produced at the same HTTs but with different sweep gas compositions (100% N_2 vs. 96% N_2/4% O_2). While the introduction of O_2 likely made a difference in the surface chemistry (See Figures 4.2 & 4.6 for evidence) of the biochar products, there was not a clear consequence of that surface change--meaning for some comparisons the sorption performance improved while for others it got worse (See Appendix D). Once more, additional experimentation not initially proposed, looking at activated carbons with known mesoporosity, will be undertaken and presented in full (partially here) in the final report.

For the sorption performance towards DOC (humic acid as surrogate), a bar graph of DOC equilibrium concentration (mg/L) for samples produced under 100% N_2 sweep gas are shown in Figure 4.5. Remembering that the two lowest HTTs (300 and 375 °C) actually release significant DOC on exposure to water (see Figure 4.1), it is possible to have a net release (not uptake) of DOC in sorption experiments. When looking at Figure 4.5, the control (far right) represents the DOC concentration when no biochar is added (no release or uptake of DOC) and has a value 3.7 mg/L. Any equilibrium DOC concentrations below 3.7 represents a net removal of DOC by the biochar product, while values above 3.7 represent a net release of DOC (unwanted). Similar to the metal sorption test results, higher values of HTT show much better performance, but for DOC removal, the clear cutoff for improved performance is slightly higher (600 °C for metals, 675 °C for DOC). While the product with an HTT of 525 °C revealed a relatively small net removal of DOC, all other samples produced ≤ 600 °C revealed a net release of DOC. It should also be noted that all biochar products produced at HTTs ≥ 675 °C had virtually identical DOC uptake performance when compared to the activated carbon sample.

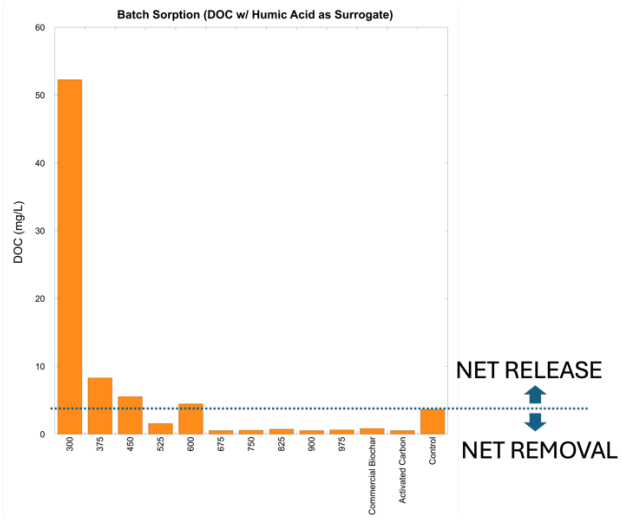

Figure 4.5 A bar graph of DOC equilibrium concentrations produced in batch sorption experiments for biochar products produce under 100% N_2 sweep gas.

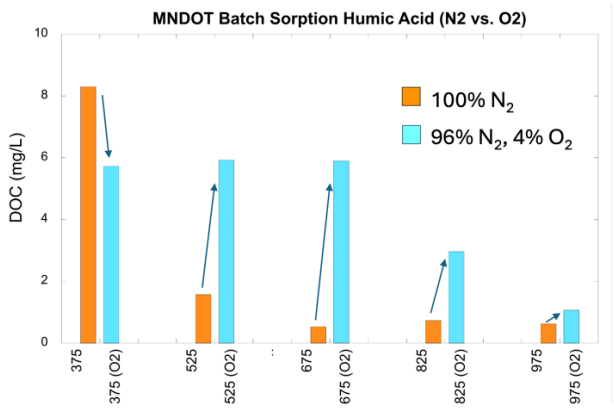

Figure 4.6 Bar graph plots of equilibrium DOC concentrations from batch sorption experiments comparing samples produced at the same HTT but under 100% N_2 sweep gas (orange) and under 96% N_2/4% O_2 (light blue).

4.3 Statistical Evaluations

Covariance reveals the tendency of a linear relationship between two random variables where a positive sign (>0 to 1) results when greater values in one variable correspond to greater values in the other and a negative sign (<0 to -1) results when greater values in one variable correspond to lesser values in the other. Covariance can be quantified by a number of different mathematical operations, but the most widely used formula gives what is referred to as "Pearson's r:"

$$r_{xy} = \frac{\sum_{i=1}^{n}(x_i - \bar{x})(y_i - \bar{y})}{\sqrt{\sum_{i=1}^{n}(x_i - \bar{x})^2} \cdot \sqrt{\sum_{i=1}^{n}(y_i - \bar{y})^2}}$$

The r value is a correlation coefficient and results from the normalization of the covariance. The absolute r value can be used to qualify the strength of the correlation as negligible (0.00 - 0.10), weak (0.10 - 0.40), moderate (0.40 – 0.70), strong (0.70 – 0.90) and very strong (0.90 – 1.00) (Schobe et al, 2018). In Figure 4.7 below, a "heat map" for Pearson's r between two variables is shown allowing for the identification of variable pairs that correlate with one another. The sorption performance towards Pb uptake could not be evaluated here because in many experiments the biochar removed Pb to concentrations below the instrument (ICP-MS) detection limit.

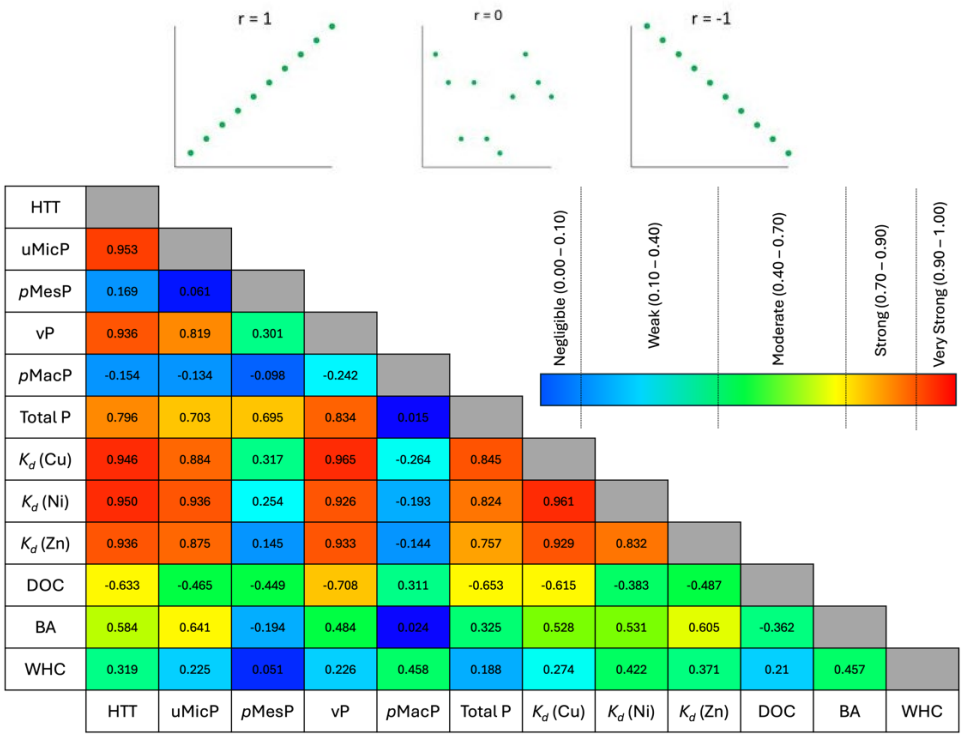

Figure 4.7 A "heat map" for Pearson's r correlation coefficients where BA and Total P, the only terms not previously defined, stand for butane activity and total pore volume (0.36 to 100, 000 nm) respectively. These r values presented here are generated from the set of 10 biochar samples produced under 100% N_2 sweep gas.

It is important to distinguish correlation from dependency, as dependency has the additional caveat of causality where correlations are agnostic to causality and can reveal a correlation between variables even if there is no true connection. For example, there might be a correlation between ice cream sales and drowning deaths, where both sales and deaths increase during summer months, but eating ice cream does not cause people to drown. In the context of this project, dependencies can only be asserted when changes in the dependent variable (response) are only influenced by a single independent variable. For example, if we wanted to see how the K_d for Cu^{2+} depends on vP we would need to be able to produce a series of biochar samples with varying vP values while keeping all other attributes of the biochar fixed. We have shown that we can produce biochars with different vPs (see Figure 5b) by changing the HTT used for production, but as we change the HTT the surface chemistry also changes which also impacts the resulting K_d responses. So, while vP is strongly correlated with Cu^{2+} K_d (r = 0.965), we cannot state that they are dependent on one another.

In other examples, we can be more confident in asserting dependency. When looking at how vP responds to HTT (r = 0.936), we can be confident that differences in vP values are a direct result of the change in HTT used and no other factors are influencing the vP response. We can the state that vP values are dependent on the HTT used for biochar production. The examination the heat map in Figure 19 can not only be useful for identifying correlations it can also be helpful to understand when variables are not correlated. The table below summarizes the key observations and corresponding interpretations:

Table 4.1. A List of Observations and their Corresponding Interpretations.

Observation	Interpretation
- uMicP vs. HTT (r = 0.953)	Biochar uMicP is dependent on HTT. Micropores are created when volatile organic compounds are liberated from the biomass due to thermal degradation. As HTT increase, more volatile compounds are liberated from the biomass.
-vP vs. HTT (r = 0.936)	Biochar vP is dependent on HTT. While the mechanism for the increasing vP is not clear, it has been speculated that at elevated HTTs vascular pores well below the particle surface breakthrough and connect with pores that reach the surface. This connection allows for increased intrusion of Hg (and therefore vP values) during MIP experiments.
-*p*MesP vs.HTT (r = 0.169) -*p*MacP vs. HTT (r = -0.154)	Both *p*MesP and *p*MacP are independent of HTT. It is well known that to increase mesoporosity of carbon-based materials, an activation agent is required which was not used in this set of biochar samples. Large macropores (larger than vascular pores) have never been shown to form during pyrolysis of biomass.
-K_d(Cu) vs. HTT (r = 0.946) -K_d(Ni) vs. HTT (r = 0.946) -K_d(Zn) vs. HTT (r = 0.946)	There is a very strong correlation between HTT and sorption performance towards all metals. We know surface chemistries change with HTT and can also impact sorption performance, so we cannot state dependency.
-K_d(Cu) vs. uMicP (r = 0.884) -K_d(Ni) vs. uMicP (r = 0.936) -K_d(Zn) vs. uMicP (r = 0..875)	There is a strong to very strong correlation between uMicP and sorption performance towards all metals. This is only a coincidence. While dissolved metal cations are small enough to fit into pores in the uMicP range, metal cations are charged and repel each other and would not collect appreciably in such tight quarters.
-K_d(Cu) vs. *p*MesP (r = 0.317) -K_d(Ni) vs. *p*MesP (r = 0.254) -K_d(Zn) vs. *p*MesP (r = 0.145)	There is a weak correlation between *p*MesP and sorption performance towards all metals. This data only considered samples produced under 100 % N_2 sweep gas and so large differences in *p*MesP values were not afforded.
-K_d(Cu) vs. vP (r = 0.965) -K_d(Ni) vs. vP (r = 0.926) -K_d(Zn) vs. vP (r = 0.933)	There is a very strong correlation between vP and sorption performance towards all metals. Since TPVs in the vP regime represent the largest values of any other regime and account for ~50% of the total pore volume, increases in vP values contribute the most to increasing the surface area of biochar. It is highly likely that surface area is a strong contributor to sorption performance. We cannot explicitly state dependency here as the surface chemistry changes must also be considered.
-K_d(Cu) vs. K_d(Ni) (r = 0.961) -K_d(Cu) vs. K_d(Zn) (r = 0.929) -K_d(Zn) vs. K_d(Ni) (r = 0.832)	There is a strong to very strong correlation between all pairs of metal sorption performances. This is logical because if a biochar product has good sorption performance towards one metal cation, it likely is also good for many other metals as well.
DOC vs vP (r = -.708)	Since DOC values go down with improved sorption performance, a negative sign is expected for r values. Similar to the metal K_d values vs. vP, there is a strong correlation between vP values and DOC sorption performance that is likely, but not definitively, due to increasing surface area upn increase in vP.
Butane Activity & WHC	There is not a strong correlation between butane activity and any of the other variable, and the same can be said for WHC.

Chapter 5: Conclusions

The primary goal for this study was to gain insight into the biochar material properties which would afford the best sorption performance toward various contaminants of concern relevant to roadway stormwater runoff. In phase 2 of this project, field-scale trials will commence, where only a couple of different biochar products can be looked at and will rely on results from this part of the project (Phase 1) to select the best biochar products to examine. In addition to identifying key physical properties, recommendations for testing will be presented here along with guidance on what acceptable test result values meet material specification requirements. When formulating the testing chart seen below, we approached it as if the biochar practitioner is completely ignorant to the nature of the biochar product, meaning the feedstock used and HTT employed, for example, are not known. The other assumption we will make is that the biochar material has not been activated. Activated carbon materials are much more expensive to produce and are not economically practical for large-scale deployment uses, such as incorporation into roadside BRSs. With that context, we have identified 3 material/production requirements which afford high sorption performance towards dissolved metals (Cu, Ni, Zn and Pb) and DOC:

Table 5.1. Table Listing the Recommended Testing (and explanations for how and why) for Consideration of Biochars to Be Used in BRSs

Property	What	Why	How
Extractives Content **(< 0.25%)**	A 50/50 benzene/ethanol solvent mixture is used to extract deposited volatile organics via Soxhlet extraction. Total extractives weight is reported as a 5 of the sample mass.	1) To ensure deploying biochar in the environment does not result in unwanted leaching of volatile organics into watersheds. 2) Deposited organics occupy surface sorption sites that could otherwise be used for contaminant sorption. 3) High extractives content can result in a net release of DOC.	While this test is not commonly offered by analytical service labs, this test does not require expensive instrumentation and can be onboarded in any chemistry lab with minimal expense.
HTT **(≥ 675 °C, H:C_{org} ≤ 0.2)**	HTT refers to the highest thermal treatment temperatures experienced by biomass upon conversion to biochar.	While significant increases in sorption performance towards metals can be achieved at HTTs ≥ 600 °C, DOC uptake requires slightly higher temperatures (≥ 675 °C) before net removal of DOC is afforded.	Biochar producers stated HTT on commercial products is not acceptable for ensuring the appropriate HTT was actually experienced by the material during production. To confirm the HTT, one must rely on testing for the H:C_{org} value which can be calculated from ultimate analysis and inorganic carbon values (aka "carbon in ash). There are several analytical service labs that can perform this test, but we recommend using TPI (Conyers, GA) as they specialize in biochar testing.

Property	What	Why	How
Vascular Porosity **(MIP, ≥ 0.40 mL/g vP, Best Option)** **(SEM, visual ID, 2nd best option)** **(WHC, ≥ 3 g/g, 3rd best option)** **(CRI, ≥ 40%, 4th best option)**	Depending on the biomass type and other factors (e.g., harvest time), the diameter of the vascular pores can vary from ~500 nm to 30,000 nm. In PSD experiments the vascular pores are easily identifiable and the pore diameter range used to calculate the vP TPV can be modified to match the diameter range of the vascular pores identified in PSD experiments.	Due to the lack of significant mesoporosity common to all non-activated biochar products, a biochar material relies on its vascular porosity to achieve performance targets.	**-MIP:** Since we are only interested in the vP range, gas adsorption experiments (N_2 and CO_2) which probe porosity in the 0-50 nm range are not required. This is the best option for ensuring vascular porosity as it allows for the quantification of this property. Many analytical service labs offer this test. **-SEM:** Although not quantitative, visually inspecting material surface morphology via SEM gives clear evidence of vascular porosity. **-WHC:** Vascular pores are right-sized for water uptake, which makes sense as the vascular network in plants is used for water transport. Materials with known lack of vP were tested here and consistently resulted in low WHCs when compared to vascular biochar products. This does not quantify the vP, but we are unaware of any carbon-based material lacking in vP that can achieve WHCs above 3 g/g. When performing WHC, fine particulate material (<20 mesh) must be avoided as small particles result in small interparticle voids which can uptake water and give inflated WHC values. **-CRI:** While this test will require a more robust data set to increase confidence in its efficacy as a proxy for total pore volume, early indications are that this may be a great alternative. Since this test, as it is currently being presented here, correlates CRI to total pore volume and not specifically for vP, the evidence is strong that it is likely the vascular pores in biochar which result in high CRI values

References

EBC (2024), European biochar certificate–guidelines for a sustainable production of biochar. *European Biochar Fondation (EBC):* Arbaz, Switzerland. (http://european-biochar.org). Version 10.4 from 20th Dec 2024.

Jagiello, J., Ania, C., Parra, J. B., & Cook, C. (2015). Dual gas analysis of microporous carbons using 2D-NLDFT heterogeneous surface model and combined adsorption data of N2 and CO2. *Carbon*, *91*, 330-337.

Junghans, U., Bernhardt, J. J., Wollnik, R., Triebert, D., Unkelbach, G., & Pufky-Heinrich, D. (2020). Valorization of lignin via oxidative depolymerization with hydrogen peroxide: towards carboxyl-rich oligomeric lignin fragments. *Molecules*, *25*(11), 2717.

Lee, B. H., Lee, H. M., Chung, D. C., & Kim, B. J. (2021). Effect of mesopore development on butane working capacity of biomass-derived activated carbon for automobile canister. *Nanomaterials*, *11*(3), 673.

Liu, K., & Ostadhassan, M. (2019). The impact of pore size distribution data presentation format on pore structure interpretation of shales. *Advances in Geo-Energy Research*, *3*(2), 187-197.

Lundy, L., Ellis, J. B., & Revitt, D. M. (2012). Risk prioritisation of stormwater pollutant sources. *Water research*, *46*(20), 6589-6600.

Moradi, N., & Karimi, A. (2021). Effect of modified corn residue biochar on chemical fractions and bioavailability of cadmium in contaminated soil. *Chemistry and Ecology*, *37*(3), 252-267.

Nguyen, B. T., Trinh, N. N., Le, C. M. T., Nguyen, T. T., Tran, T. V., Thai, B. V., & Le, T. V. (2018). The interactive effects of biochar and cow manure on rice growth and selected properties of salt-affected soil. *Archives of Agronomy and Soil Science*, *64*(12), 1744-1758.

Nguyen, T. H., Cho, H. H., Poster, D. L., & Ball, W. P. (2007). Evidence for a pore-filling mechanism in the adsorption of aromatic hydrocarbons to a natural wood char. *Environmental science & technology*, *41*(4), 1212-1217.

Omara, P., Singh, H., Singh, K., Sharma, L., Otim, F., & Obia, A. (2023). Short-term effect of field application of biochar on cation exchange capacity, pH, and electrical conductivity of sandy and clay loam temperate soils. *Technology in Agronomy*, *3*(1).

Schober, P., Boer, C., & Schwarte, L. A. (2018). Correlation coefficients: appropriate use and interpretation. *Anesthesia & analgesia*, *126*(5), 1763-1768.

Thommes, M., Kaneko, K., Neimark, A. V., Olivier, J. P., Rodriguez-Reinoso, F., Rouquerol, J., & Sing, K. S. (2015). Physisorption of gases, with special reference to the evaluation of surface area and pore size distribution (IUPAC Technical Report). *Pure and applied chemistry*, *87*(9-10), 1051-1069.

Varadachari, C., & Ghosh, K. (1984). On humus formation. *Plant and Soil*, *77*, 305-313.

Xiong, J., Liang, L., Shi, W., Li, Z., Zhang, Z., Li, X., & Liu, Y. (2022). Application of biochar in modification of fillers in bioretention cells: A review. *Ecological Engineering*, *181*, 106689.

Appendix A.
Biochar Characterization Plan From Proposal

Task 4 (Biochar Characterization): Each biochar sample produced in Task 3 will be characterized in 6 different analyses. The analyses will include a) proximate and ultimate analysis (duplicate), b) complete pore size distribution (single replicate), c) butane activity (single replicate), d) water holding capacity (triplicate), e) cation exchange capacity (triplicate) and f) extractives quantification (single replicate). Additionally, if any of the biochars produced are deemed to present contamination risks (creosote impregnated railroad ties used as feedstock e.g.), their extractives will be further analyzed to identify the chemical constituents via gas chromatography-mass spectrometry. Results from each of these analyses will be assessed relative to their pyrolysis conditions in order to determine how the process affects the physical properties of the resulting biochars.

Proximate and ultimate analyses will be performed on each raw biomass feedstock as well as all biochar products. Proximate analysis will produce quantifications of total moisture (ASTM E871), total ash (ASTM D1102), volatile matter (ASTM D3175) and fixed carbon (ASTM D3172) while ultimate analysis will quantify elemental compositions (weight %) of carbon (ASTM D5373), hydrogen (ASTM D5373), nitrogen (ASTM D5373) and oxygen (ASTM D3176). From this data we can determine the degree of carbonization in biochar products by looking at the hydrogen to organic carbon molar ratios ($H:C_{org}$) and by examining the carbon content (both fixed carbon from proximate and %C from ultimate) of both the raw biomass and resulting biochars. This will be used to determine the number of CORCs that can be produced per mass of biochar on a sample-by-sample basis.

Complete pore size distributions (PSDs) will be generated for all biochar samples by combining results from nitrogen adsorption, carbon dioxide adsorption and mercury intrusion porosimetry experiments. This type of pore structure analysis provides the most accurate and complete picture of the surface morphology and produces reliable, reproducible results (Jagiello 2015). Biochar sorption performances for metals and hydrophobic organics (chosen contaminant classes for Task 5) have shown to be dependent upon the porosity and as such PSDs are critical physical properties to evaluate (Kaya 2022). Biochar samples produced from plant biomass typically contain narrow micropores (< 1 nm in diameter) and due to kinetic restrictions at 77K (requisite experimental temperature), nitrogen is not a suitable adsorbent for micropore analysis. Specific surface area (SSA) is most often assessed using nitrogen (BET analysis) and it has been determined that for microporous biochars, this method is not appropriate (Thommes 2015). A potential drawback of complete PSD analysis is that it may be cost prohibitive and because of this potential we propose to perform a much faster and affordable analysis, butane activity (ASTM D5742-16), as well. Complete PSDs allow for user-defined regime (2.3 to 5.1 nm e.g.) pore volumes to be calculated and correlations between butane activity and various pore size regimes to be explored. If correlations arise, it may be possible to substitute butane activity for complete PSD in the final specification criteria recommendations.

Changes in soil water holding capacities due to biochar amendments can be predicted from assessing the water holding capacity of the biochars used in the amendment. Increases in soil water holding capacities have shown to increase drought resistance, improve soil microbial community health and increase soil nutrient retention, all positive attributes for improved plant growth in BRSs (Yu 2013). All biochar samples will be analyzed for the water holding capacities (ISO 14238 Annex A) and will inform

decisions made for which biochar samples should be recreated for greenhouse plant growth studies (Phase 2 of project).

While the sorption mechanism for many COCs can be attributed to weak surface interactions (π-π and Van der Waals interactions e.g.) where sorption capacities directly correlate to PSDs, some cationic COCs (metals e.g.) can be exchanged for hydrogen cations found on biochar surfaces and it has been found that cation exchange capacity (CEC) measurements are the most important trait for determining the ability of biochar to stabilize metals through sorption-based interactions (Guo 2020). For this reason, we plan to assess the CECs (amended AOAC 973.03, Rippy 2007) of all biochars samples and compare them with metal sorption performances from Task 5.

For most applications, a BRS being no exception, it is desirable to produce a "clean" biochar product with a minimal amount of mobile or extractable organic material. Residual mobile organic byproducts (tars) of biomass pyrolysis can remain adsorbed to the surfaces of biochars if pyrolysis conditions are suboptimal. Examples of suboptimal conditions could be inefficient heat transfer in the kiln, too short of residence times or inadequate gas draw. Depending on the feedstock choice and pyrolysis conditions, some of the chemicals found in the mobile organics are considered toxic (polycyclic aromatic hydrocarbons e.g.). By extracting the biochar in overnight Soxhlet experiments with a mixture of benzene and ethanol, the weight % of mobile organics can be quantified allowing for a quick evaluation of the kiln performance.

Appendix B.
Additional Proximate and Ultimate Analysis Plots

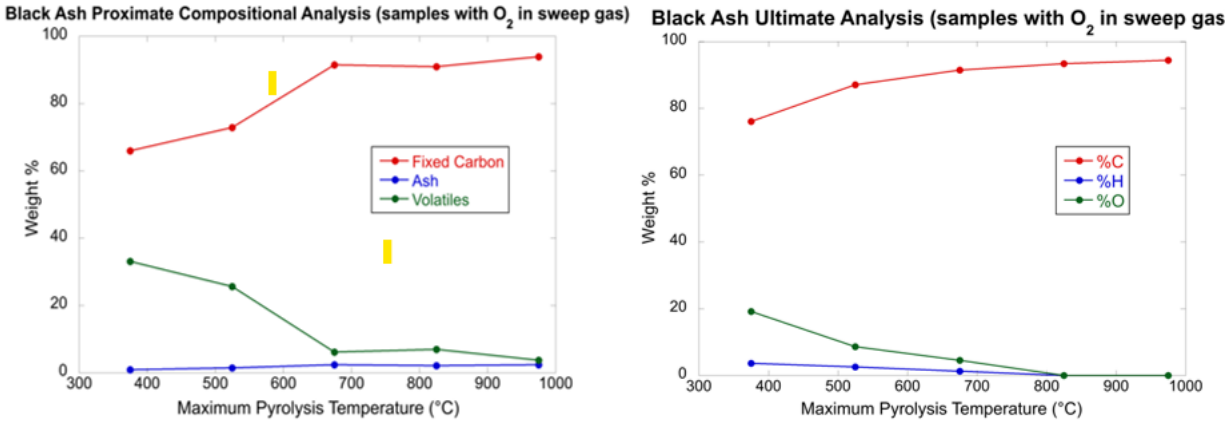

Figure B-1. Plots of Proximate and Ultimate data vs. HTT for set of 5 biochar products produced under 96% N2/4% O2 sweep gas.

Appendix C.
K_d Batch Sorption Results (100% N_2 Only)

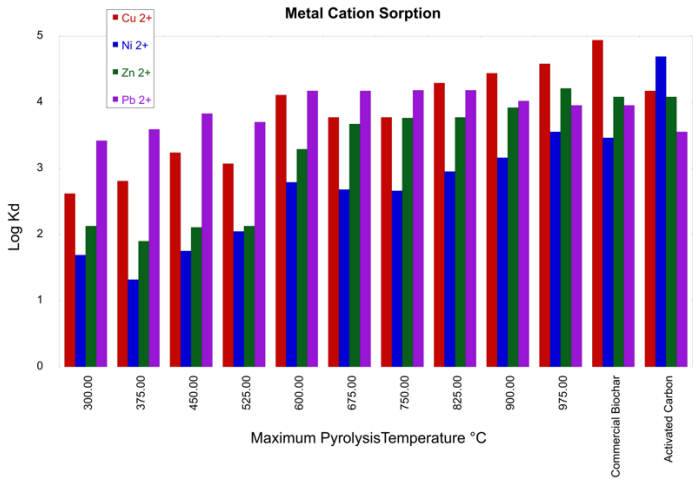

Figure C 1. Bar graph plot for the log Kd values produced for batch sorption tests for 4 contaminant metals (Cu = red, Ni = blue, Zn = green, Pb = purple) using biochars produced under 100% N2 sweep gas.

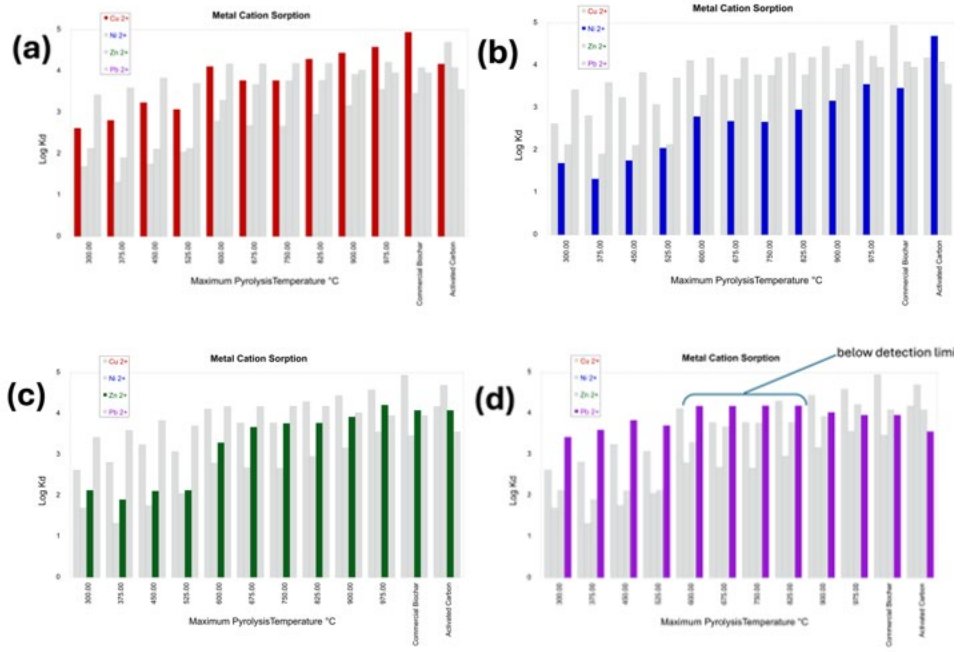

Figure C 2. Bar graph plots for log K_d values highlighting sorption performance towards Cu (a), Ni (b), Zn (c), and Pb (d).

Appendix D.
Normalized Concentration Batch Sorption Results (100% N_2 vs. 96% N_2/4% O_2)

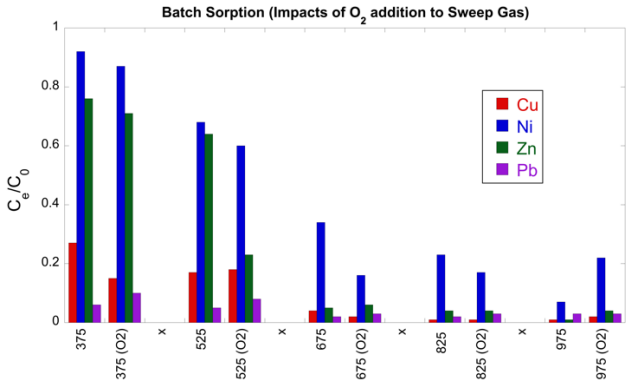

Figure D 1. Bar graph plots of normalized concentration results from batch sorption experiments comparing samples produced at the same HTT but under 100% N2 sweep gas (left) and under 96% N2/4% O2 (right).

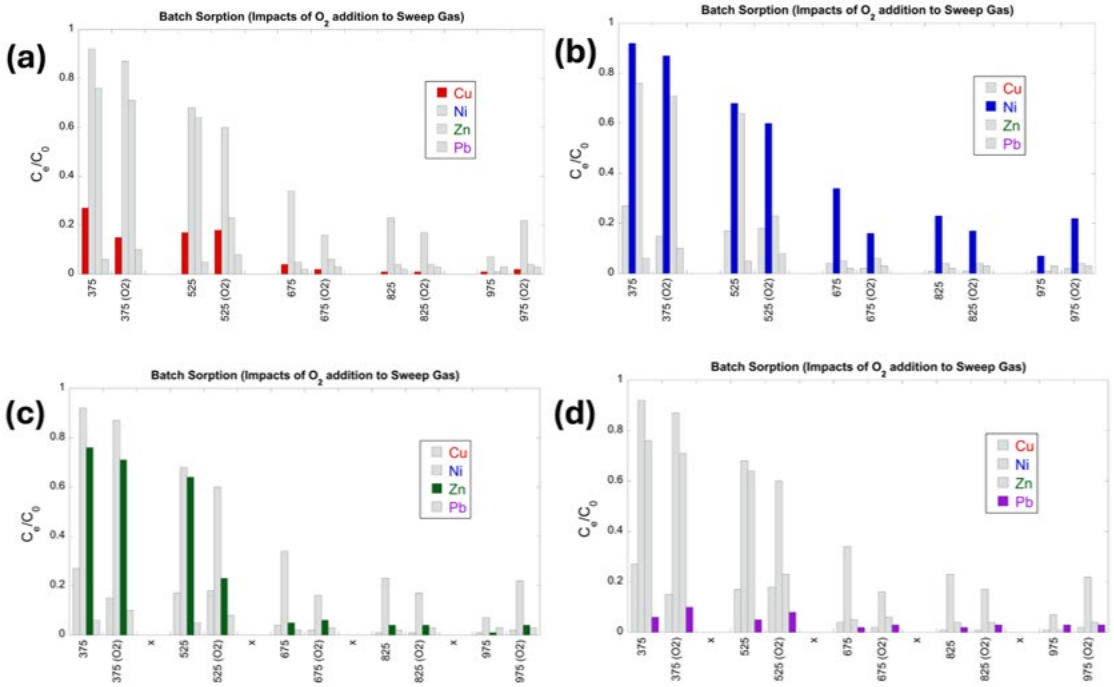

Figure D 2. Bar graph plots of normalized concentration results from batch sorption experiments comparing samples produced at the same HTT but under 100% N2 sweep gas (left) and under 96% N2/4% O2 (right) highlighting results from Cu (a), Ni (b), Zn (c)